WHP Cruise Summary Information

WOCE section designation	A12
Expedition designation (EXPOCODE)	06AQANTX_4
Chief Scientist(s) and their affiliation	Peter Lemke, AWI
Dates	1992.05.21 – 1992.08.05
Ship	POLARSTERN
Ports of call	Cape Town, South Africa to Puerto Madryn, Argentina
Number of stations	115
Geographic boundaries of the stations	34°07.0''S 58°25.0''W 17°58.0''E 70°49.0''S
Floats and drifters deployed	6 drifters
Moorings deployed or recovered	none
Contributing Authors In order of appearance	R. Brandt W. Frieden T. Rothe O. Schulze M. Thomas S. Mai T. Viehoff S. Rasenat W. Dierking M. Drinkwater A. Bochert C. Garrity M. Schröder A. Wisotzki N. Brunken I. Hansen P. Heil M. Kreyscher S. Moschner N. Steiner U. Sterr K. U. Richter H. Diedrich K. Bulsiewicz W. Plep H. Rose J. Sultenfuss J. M. J. Hoppema J. J. M. Belgers

WHP Cruise and Data Information

Instructions: Click on items below to locate primary reference(s) or use navigation tools above.

Cruise Summary Information	**Hydrographic Measurements**
Description of scientific program	CTD - general
Geographic boundaries of the survey	
Cruise track (figure)	
Description of stations	
	Salinity
Floats and drifters deployed	Oxygen
Moorings deployed or recovered	Nutrients
	CFCs
Principal Investigators for all measurements	Helium
Cruise Participants	Tritium
Problems and goals not achieved	CO2 system parameters
Other incidents of note	Other parameters
Underway Data Information	**Acknowledgments**
Navigation	**References**
Bathymetry	
Acoustic Doppler Current Profiler (ADCP)	**DQE Reports**
Thermosalinograph and related measurements	
XBT and/or XCTD	CTD
Meteorological observations	S/O2/nutrients
Atmospheric chemistry data	

Preliminary cruise report
May 15, 1995

A. Cruise narrative

A.1.a WOCE designation SR2, SR4

A.1.b EXPOCODE 06AQANTX/4

A.1.c Chief scientist

Peter Lemke
Alfred Wegener Institut fuer Polar und Meeresforschung
Postfach 1201061
Am Handelshafen 12
D-27515 Bremerhaven
Germany
Telephone: +49-471-4831-512
Telefax: +49-471-4831-425

A.1.d Ship Polarstern

A.1.e Ports of call Cape Town, South Africa to Puerto Madryn, Argentina

A.1.f Cruise dates May 21 to August 5, 1992

A.2 Cruise Summary

A.2.a Geographic boundaries

The first section (A12) from Cape Town to Antarctica began at 34˚16'S 7˚20'E and proceeded southwest from there to 4˚S 0˚E and then followed the Greenwich Meridian to 69˚42'S. After the work around Antarctica was complete the repeat section, SR04, was begun at 70˚31'S 9˚9'W and proceeded northwest through the Weddell Sea to finish at 61˚S 58˚25'W.

A.2.b Stations occupied

The section A12 along the Greenwich Meridian consisted of 71 deep casts and 8 biological casts to 300m depth. The section SR04 across the Weddell Sea included 28 full depths and 6 biological casts to 300m depth. For calibration 2 deep casts were taken. The oceanographic program included 101 casts of full hydrographic work. Each cast included 24 water samples of temperature, salinity, oxygen, silicate, phosphate, nitrate, nitrite and 14 special biological casts. Additional tracer measurements were done including tritium, helium, chlorofluorocarbons F-11 and F-12, and oxygen isotopes ^{18}O and ^{16}O.

A.2.c Floats and drifters deployed

On 10 and 11 July six drifters (Metocean) in one array took place. Deployment positions of these drifters are given in Table 6. Two small drifters, measuring only air pressure and air temperature, and two highly instrumented drifters were deployed at a distance of 70km to each other along the track of the vessel. Two additional small drifters were placed by helicopter in a position nearly 70km away perpendicular to the ship's track. The two central drifters are measuring the air pressure, the air and the sea surface temperature, the snow height and ice temperature profiles with an ice thermistor string. Under these central drifters a 250m long underwater thermistor cable is fixed with 30 thermistors and also two sensors, measuring pressure, temperature, conductivity and salinity of the water in 50m and 250m depth. All drifters use the ARGOS system for data transmission.

A.2.d Moorings deployed or recovered

On the long ice station a mobile system of current meters was used from a sea ice floe. A six hour long time series with a fixed acoustic current meter 1.5m below the sea ice was taken to measure the turbulent fluctuations of velocity and temperature in the oceanic boundary layer. The objective of this experiment was to investigate whether a rigid construction can be used to measure physical signals due to Karman vortices around the instrument, without too much noise in the interesting frequency band. The launch and recovery of the instrument through a 10cm hole through 2.0m of ice led to unforeseen difficulties that greatly reduced the measurement time. Radar reflectors (Table 5) were deployed to aid ice-tracking capabilities.

A.3 List of Principal Investigators:

Measurement	Principal Investigator	Institution
Salinity	M. Schröder	AWI
Oxygen	M. Schröder	AWI
Oxygen isotopes	M. Schröder	AWI
Nutrients	G. Kattner	AWI
CFCs	W. Roether	UNIB
Helium/tritium	W. Roether	UNIB
CTD	M. Schröder	AWI
Neon	---------	
TCO_2	J.M.J. Hoppema	NIOZ/AWI
XBTs	M. Schröder	AWI
Meteorology	W. Frieden	IMH
Bathymetry	---------	
ADCP	M. Schröder	AWI
Remote sensing	T. Viehoff	AWI
Marine Geology	C. Haas	UNIK
Biological program	E.-M. Nöthig	AWI

A.4 Scientific Programme and Methods

Cruise Summary Information Itinerary: The expedition ANTX/4, the Winter Weddell Gyre Study 1992 (WWGS-92), consisted of two hydrographic sections of the World Ocean Circulation Experiment (WOCE), during which vertical profiles of temperature, salinity, oxygen, CO_2, nutrients and several tracers (tritium, ^{3}He, He, ^{18}O, ^{16}O, Ne, Freon-11 and Freon-12) were taken. These activities represented the largest part of the oceanographic program. The first section (A12) from Cape Town to Antarctica mainly followed the Greenwich Meridian. The second section (SR04), a traverse of the Weddell Gyre, extended from Kapp Norvegia to King George Island. The section SR04 was taken for the third time after September 1989 and December 1990 cruises and, therefore, allows estimates of the variability of the water mass production in the southern Weddell Sea. The main goals of the oceanographic program were the determination of the baroclinic mass transport from the horizontal heat and salt fluxes in the Antarctic Circumpolar Current and in the Weddell Gyre, and the water mass modification in the southern Weddell Sea. For both sections the oceanographic measurements represent the first midwinter realization.

Polarstern left Cape Town on 21 May 1992 with 42 crewmembers and 45 scientists aboard. The oceanographic program started on 22 May in the morning a few miles southwest of Cape Town with the beginning of the section A12. Stations were taken with a distance of 30 to 45nm. Above the continental shelf slopes the station distance was smaller depending on given depth intervals.

In the beginning the course led southwest to the Greenwich Meridian passing the subtropical front on 27 May at 40˚25'S, 10˚50'E and the subpolar front on 2 June at 45˚50'S, 01˚04'E. Above the Shannon Seamount (42˚59.6'S, 2˚20.3'E) two pressure gauges were deployed at a depth of about 800m. Steaming south along the Greenwich Meridian the first icebergs were sighted on 3 June at 47˚30'S. On 5 June Polarstern crossed the polar front at 51˚30'S. North of the polar front the biology program started with a daily bongo- or multi-net tow.

The ice edge was crossed on 12 June at 60˚56.4'S. The sea ice was mainly pancake and grease ice up to 68˚S where the ice got thicker and more compact. Here the work of the sea ice and remote sensing group started on the ice floes on 17 June.

On 16 June the sun set for the polar night. Nevertheless, helicopter work was generally possible for two hours during the twilight at noon for taking snow and ice samples or obtaining data from the infrared line scanner or the laser altimeter in the vicinity of the ship.

The section A12 was completed on 19 June with the 71st station off the shelf ice at 69˚42.6'S, 0˚40.8'W. Polarstern steamed through the freezing coastal polynya towards Neumayer-Station Entering Atka Bay on 20 June the weather conditions deteriorated such that a supply of the station with helicopter or skidoo was impossible. A depot was put on

the sea ice, which was visited from the station later during calm weather. Polarstern tried to leave Atka Bay but the pressure in the sea ice cover due to the strong easterly winds was too high. It was only after a turning of the wind to southeast on 29 June that Polarstern was able to escape the dense pack ice in Atka Bay and steam towards Kapp Norvegia.

After finishing a CTD station off Kapp Norvegia on 1 July a hurricane stopped the continuation of the section towards the northwest. Polarstern was forced to shut off the engines, and drifted due to continuing strong northeasterly winds passively with the sea ice in the coastal current 140nm to the southwest. After a turning of the wind towards southwest on 8 July the ship escaped the coastal current. On course to the center of the Weddell Gyre six ARGOS-equipped drifters and ten radar-reflectors were deployed on 10 and 11 July between 69˚44'S, 23˚47'W and 68˚15'S, 27˚35'W.

The polar night ended on 11 July. The section work continued on the planned cruise track on 13 July. Polarstern now entered regions with increased concentration of multiyear sea ice with the thickness of 150 to 250cm. The temperature decreased to 32˚C such that most leads were frozen. The average speed of the icebreaker reduced to 2 knots. Considering the remaining time and fuel it was decided on 19 July to leave the planned cruise track in northward direction following the lead pattern towards South Orkney.

On the shelf southeast of South Orkney a three day long ice station took place from 21 to 24 July. The oceanographers performed turbulence measurements in the mixed layer under the sea ice. Besides the general program of measuring sea ice and snow thickness and profiles of temperature, salinity and porosity, the sea ice group investigated the elasticity of the ice floe - and hence its thickness - with seismic methods. The remote sensing group was glad to view the same piece of sea ice with their sensors under different weather conditions. The meteorologists were able to collect a longer data set for the energy balance at the sea ice surface. The first part of the station took place under cold conditions (-22˚C). Then a passing warm front with Beaufort 10 winds raised the temperature up to the freezing point.

After the long station Polarstern steamed westward north of South Orkney taking CTD stations in order to determine the baroclinic flow between South Orkney and Elephant Island. The last CTD station was taken on 30 July 1992 above the South Shetland Trench north of King Polarstern George-Island at a water depth of 5200m. This station with a Freon (tm) blank at depths between 2000 and 3000m was used for calibration of the tracer data. A total of 115 stations were taken during the cruise.

The meteorological program focused on the energy balance at the sea ice surface. The activities consisted of the determination of the short- and long-wave radiation balance, the turbulent fluxes of momentum, sensible and latent heat, and the heat conduction through snow and sea ice. The vertical structure of the entire troposphere was determined from radio sonde ascents. Six ARGOS-equipped drifters were deployed, two of which also measured the vertical temperature profiles in atmosphere, snow, ice and upper ocean, snow accumulation and salinity at two depths, in addition to position, air pressure and air

pressure tendency. The goal of the meteorological program was the determination of the thermodynamic and dynamic boundary conditions for sea ice growth and motion.

One of the main components of the expedition was the remote sensing ground truth program for the Synthetic Aperture Radar (SAR) and the Along Track Scanning Radiometer (ATSR) of the European satellite ERS-1, and four infrared, visible and microwave channels of sensors on other satellites. Data of a Real Aperture Radar (RAR) on board a satellite of the Russian OKEAN series could not be received as planned since a replacement for the defective OKEAN-3 satellite was not launched in time.

Emission, reflection and scattering properties of the sea ice surface were determined with infrared and microwave radiometers and with a scatterometer. Ground truth data of sea ice concentration were obtained with a line-scan camera operated from a helicopter. The sea ice surface topography (pressure ridges) was measured with a helicopter-borne laser altimeter. The main goal of the remote sensing program was the improvement of algorithms for determining sea ice concentration, motion, ice type and surface roughness on larger scales in space and time. These data sets are required to improve our understanding of the physics of sea ice and to provide observations to test and verify sea ice models.

Measurements of the physical properties of snow and sea ice included the sea ice thickness, vertical profiles of density, salt, temperature, pore size, and texture, and the dielectric constant and small-scale (mm-cm) surface roughness. These data will be used to better interpret satellite observations. Finally, a first attempt was undertaken to determine sea ice thickness with a seismic multi-frequency reflection method.

The main goal of the biological program was the plankton ecology within the sea ice and the upper ocean. Measurements of the distribution of phyto- and zooplankton, of particulate organic carbon and nitrogen and of chlorophyll-a were taken, and were compared to the properties of the oceanographic environment.

The chemical measurements consisted of lipid investigations undertaken to obtain information on the physiological adaptation of copepods, which represent a large fraction of the biomass in the Southern Ocean, with respect to environment and nutrient supply.

Within the geological program surface sediments were investigated between Cape Town and the sea ice edge using a mini-corer fixed under the CTD-rosette. Data from these samples represent the basis for paleo-oceanographic and paleo-climate re-constructions.

From the sea ice edge up to the Argentinean shelf 23 XBT-profiles were taken, and the vertical current shear was recorded continuously with an Acoustic Doppler Current Profiler (ADCP).

During the cruise 170 infrared images of the Weddell Sea region from US weather satellites were recorded. At the German receiving station at O'Higgins 400 passes of the ERS-1 SAR were received. Furthermore, after the cruise daily microwave images of the

SSM/I will be available. From the comparison of the different sensors an improvement of the algorithms for sea ice concentration and motion are expected.

On 5 August 1992 at 6:00 GMT Polarstern arrived at Puerto Madryn as planned.

A.5 Major Problems and Goals Not Achieved

After the last CTD station Polarstern steamed into Maxwell Bay off the Chilean station "Teniente Marsh", where the crew of the German ERS-l receiving station was supposed to board the ship. Unfortunately, the weather was bad. The flight from O'Higgins was cancelled, and Polarstern had to leave for Puerto Madryn without taking the crew aboard.

A.6 Other Incidents of Note

None noted.

A.7 List of Cruise Participants Cruise

TABLE 2: Cruise participants

Name	Institution
Belgers, Jan J.J.M.	NIOZ
Bochert, Axel	AWI
Brandt, Rudiger	IMH
Brey, Heinz	HSW
Brunken, Nicole	AWI
Büchner, Jürgen	HSW
Bulsiewicz, Klaus	UNIB
Dierking, Wolfgang	AWI
Dietrich, Helmut	AWI
Drinkwater, Mark	JPL
Ewald, Horst	HSW
Fahl, Kirsten	AWI
Frieden, Wolfgang	IMH
Garrity, Caren	AWU/AES
Haas, Christian	UNIK
Hansen, Imke	AWI
Heil, Petra	AWI
Holsbeek, Ludo	VUB
Hoppema, Mario	NIOZ
Jahn Petra	AWI
Köhler, Herbert	SWA
Kreyscher, Martin	AWI
Lemke, Peter	AWI

Name	Institution
Lohanick, Alan	NRL
Massom, Robert	GSFC
Mai, Stephan	AWI
Moschner, Stephan	AWI
Nöthig, Eva-Maria	AWI
Plep, Wilfried	UNIB
Rasenat, Steffen	AWI
Richter, Klaus-Uwe	AWI
Riewesell, Christian	HSW
Röd, Erhard	SWA
Rose, Henning	UNIB
Rothe, Thomas	IMH
Schröder, Michael	AWI
Schulte, Christian	AWI
Schulze, Olaf	IMH
Spiridonov, Vasili	AARI
Steiner, Nadja	AWI
Sterr, Uta	AWI
Sültenfuß, Jurgen	UNIB
Thomas, Markus	IMH
Viehoff, Thomas	AWI
Wisotzki, Andreas	AWI

Participating Institutions

Abbreviation	Address
Federal Republic of Germany	
AWI	Alfred-Wegener-Institut fur Polar- und Meeresforschung
	Postfach 12 01 61
	27515 Bremerhaven
HSW	Helicopter Service Wasserthal GmbH
	Katnerweg 43
	D-22393 Hamburg
IMH	Institut fur Meteorologie und Klimatologie der Universitat Hannover
	Nienburger Strasse 6
	30167 Hannover
UNIB	Universitat Bremen
	Bibliothekstrasse
	28334 Bremen

Abbreviation	Address
UNIK	Universitat Kiel
	Institut fur Geophysik
	Leibnizstrasse
	2418 Kiel
SWA	Seewetteramt
	Deutscher Wetterdienst
	Bernhard-Nocht-Str. 76
	20359 Hamburg
Belgium	
VUB	Vrije Universiteit Brussels
	Laboratory for Ecotoxicology
	Pleinlaan 2
	B-1050 Brussel
Canada	
AES	AES/Cress Microwave Group
	Petrie 214-York University
	4700 Keele Street
	North York, Ontario
	Canada M3J 1P3
Netherlands	
NIOZ	Nederlands Instituut voor
	Onderzoek der Zee
	P.O. Box 59
	1790 Ab den Burg, Texel
Russia	
AARI	Arctic and Antarctic Research Institute
	38 Bering Street
	19226 St. Petersburg
United States of America	
NRL	NOAA Research Laboratory
	72 Lyme Road
	Hanover, NH 03755
GSFC	NASA/Goddard Space Flight Center
	Laboratory for Oceans, Code 61
	Greenbelt, Maryland, 20771
JPL	Jet Propulsion Laboratory
	4800 Oak Grove Drive
	Pasadena, CA 91109

B. Underway Measurements

B.1 Navigation and bathymetry

B.2 Acoustic Doppler Current Profiler (ADCP)

En route measurements of velocity profiles with a ship-mounted 150kHz RDI ADCP in ice-free regions along the Greenwich Meridian (2090nm) and across the Drake Passage (680nm) were made.

B.3 Thermosalinograph and underway dissolved gasses

En route registration of surface temperature and salinity with a vessel-mounted thermosalinograph (only in regions without sea-ice cover) was done.

B.4 Expendable bathythermograph and salinity measurements

Crossing Drake Passage hourly type T7 XBTs, for a total of 23, were launched after leaving the ice edge. These data provide useful information in connection with previous XBT-cruises and with en route registrations of the ADCP which were run as far as 52˚N to calibrate the system via bottom tracking. ***XBT locations are needed CEC****

B.5 Meteorological observations

R. Brandt, W. Frieden, T. Rothe, O. Schulze, M. Thomas, S. Mai

The main objective of the meteorological program was the investigation of the ice/atmosphere interaction in midwinter. The program consisted of the determination of all components of the energy budget at the sea-ice surface during longer ice stations and short period measurements of the turbulent fluxes of sensible heat and momentum at different locations for different surface conditions (ice concentration, flow-size distribution, snow- and ice-thickness).

Particular attention was focused on the spatial variability of the energy balance components over larger leads and polynyas as a ground truth information for the validation of ERS-1 data. Additionally, aerological soundings were taken to obtain information about the vertical thermodynamic and kinematic structure of the boundary layer and the upper atmosphere.

Energy budget:

For the determination of the energy budget the following parameters were measured: the radiation budget, the turbulent fluxes of sensible and latent heat and the conductive heat flux through the snow/ice cover. In ice-covered areas the turbulent flux of latent heat can generally be neglected. In regions of thin ice or open water this part of the heat flux was estimated using the appropriate bulk formula and ship-borne humidity measurements.

a) Radiation budget

The measurements of incoming short wave and long-wave radiation have been realized with a pyranometer (CM- 11, Kipp+Zoenen) and a pyrgeometer (Eppley) mounted at the ships boom. The outgoing long-wave radiation was calculated from the radiation temperature measured with a radiation thermometer (KT-4). The albedo of the surface was also measured with a pyranometer (CM- 11).

All these measurements, except for albedo, were performed continuously beginning on 12 June, when the ship reached the ice edge and ending on July 29. The albedo measurements were only made from time to time in periods when the sun was rising above the horizon (12-17 June, 11-29 July). Due to problems with the data-logger five days of data were loss. In addition to the measurements with the KT-4 the outgoing long-wave radiation was measured also with a pyrgeometer (Eppley) during the 3 day station from 21-24 July near the South Orkneys. This additional data set allows a calibration of the KT-4 measurements. During the long ice station all instruments were installed on a sledge, placed on the ice floe in vicinity of the vessel.

As an example, four components of the radiation budget during the long ice station were plotted. The curves demonstrate the dependence of the different components on the cloud cover: a clear sky from the beginning of the station until the afternoon of 22 July and a following warm front passage with an overcast sky until the end of the station, except for 4 hours during the night from 23 - 24 July.

Fig. 2.2-2 contains the net short- and long-wave radiation as well as the total net radiation during the long ice station. Under clear sky conditions the ice surface loses up to 80W/m^2 whereas for overcast sky the components compensate each other and no net radiation energy is available at the surface.

b) Turbulent fluxes

The vertical turbulent fluxes of sensible heat and momentum were derived from wind and temperature fluctuations measured during most stations with a sonic-anemometer-thermometer (Metek) at the ship's boom (sampling frequency 10Hz). Most of the stations lasted several hours from which we finally got 38 short period data sets. The measurements were obtained over a variety ice conditions like Nilas, Pancake-ice, first-year-ice and over open water. Two longer time series were collected during the drifting periods when the ship was stuck in the ice in Atka Bay and south of Cape Norwegia. The most important data set was obtained from the 3-day station south of the South Orkneys.

In Figs. 2.2-3 and 2.2-4 the turbulent fluxes of sensible heat and momentum during the long ice station from the 21-24 July (10 minute averages) are displayed. The turbulent flux of sensible heat is highly correlated with the air temperature and the cloud conditions. Due to the clear sky and very low temperatures at the beginning of the station the heat flux to the surface was very small (positive values denote an energy gain, negative an energy loss at the surface). The energy gain increased with rising temperatures and an overcast sky up to 60W/qm. The sudden and sharp decrease in the morning of the 24

July is due to the clear sky in the night. The turbulent flux of momentum depends on the surface conditions and mainly on the wind speed.

c) Conductive heat flux through the ice

For the calculation of the conductive heat flux a newly developed thermistor stick was put into the ice during the 3-day station to obtain a time series of temperature profiles. This thermistor stick allowed the simultaneous determination of the ice temperature at seven depth levels ranging from 5cm to 1.0m below the ice/snow interface. The sampling rate during the measurements was one minute.

First results are shown in Fig. 2.2-5. The profiles chosen illustrate the influence of the air temperature on the temperature in the upper layers of the ice. During the station the air temperature rose from –22˚C to about 0˚C. Simultaneously the ice temperature in the first few centimeters increased from –21˚C to –5˚C. Moreover the profiles show that at the end of the station the temperature at a depth of 0.5m was about 2K higher than at the beginning. The light air temperature drop in the night from 23 - 24 July was not very pronounced in the ice as can be seen in the profiles.

From the temperature gradient the heat flux can be calculated using the thermal conductivity of the ice, which is mainly a function of the salinity. Salinity profiles will be available from the sea ice group.

A first rough estimation of the energy budget, containing the radiation budget Q and the turbulent flux of sensible heat, H, at the long ice station. In the beginning of the station the surface loss was nearly 50W/m^2. This energy had to be supplied by freezing processes at the bottom of the ice, which finally had to be transferred to the surface of the sea ice by the conductive heat flux. Later during the station, when the air temperature had increased and the sky was overcast, the surface received about 20 to 30W/m^2 from the atmosphere.

Radio soundings

In order to get information about the meteorological conditions in the boundary layer and the upper atmosphere a total of 169 radio soundings were performed. Within the sea ice covered region four soundings per day were taken. As an example of this extensive data set Fig. 2.2-7 shows the wind direction and the wind speed in the lower stratosphere compared to those at the surface level (all soundings at 12:00 UTC from 23 May - 27 July). The mean wind direction in the lower stratosphere is around 270, while at the surface level two main directions are visible. The more westerly directions were measured in open water and in the subtropical zone; the eastward components are mainly due to the katabatic surface winds near the antarctic continent.

Storm events

During this winter cruise five marked storm events occurred which had a strong influence on the ship's operations and the scientific work. The first storm developed on 4/5 June at 50˚S, 0˚E with 11 Beaufort winds. The cyclogenesis was driven by advection of positive

vorticity at the polar front, and the wind was geostrophically balanced. During the storm Polarstern had to stop all station work and was forced off course. The second storm event (22 June, 10 Beaufort) confined Polarstern to Atka Bay. This time the wind speed could not be explained by geostrophy alone, but by an additional strong katabatic wind component. The third storm (1 July, 12 Beaufort) forced Polarstern off course into the densely packed coastal current. This storm was basically in geostrophic balance. Only the gusts of up to 85 knots were probably katabatically induced.

The fourth storm event (23 July, 10 Beaufort) showed a typical cyclogenesis in the western Weddell Sea influenced by low pressure systems dissolving at the Antarctic Peninsula. This storm was associated with a warm front that initiated a strong temperature change during the long ice station. The fifth storm (31 July, 10 Beaufort) which seemed to be orographically induced was mainly responsible for the failure to take the crew of the German receiving station aboard. A summary of the weather conditions during the expedition is shown in Table 3 and Table 4.

TABLE 3:
Extrema of several meteorological parameters measured during WWGS-92:

Parameter	Maximum/date	Minimum/date
air pressure	1016.1 hPa/22.07	961.2 hPa/11.06
air temperature	1.1 C/25.07	-32.0 C/ 14.07
wind speed (10 minute mean)	64.3 kn/01.07	
Maximum air pressure decrease:	01.07. - O2.07. 47 hPa in 32 hours (1009 hPa to 962 hPa)	
Maximum temperature rise:	17.07. 23.4 K in 27 hours (-24.6 C to -1.2 C)	
Maximum temperature decrease:	22.06. 18.3 K in 11 hours (-5.0 C to -23.3 C)	

TABLE 4:
Temperature statistics for the cruise track within the ice cover:

Number of days with minimum < 0.0˚C: 46
Number of days with maximum < 0.0˚C: 42
Number of days with minimum < -10.0˚C: 38
Number of days with minimum < -20.0˚C: 21
Number of days with minimum < -30.0˚C: 2
Number of days with maximum < -10.0˚C: 23
Number of days with maximum <-15.0˚C: 14
Number of days with maximum < -20.0˚C: 6

B.6 Atmospheric chemistry

B.7 Remote Sensing

Several remote sensing techniques including optical, infrared and passive microwave sensors as well as active microwave instruments were applied to sea ice investigations. The main scientific aim was to link geophysical characteristics of Weddell Sea ice signatures obtained from various remote sensing instruments. These investigations serve as a basis for the interpretation of remotely sensed data in terms of sea ice variables needed in such a way that signatures may be inverted to extract key ice parameters. These ice properties are sought as primary inputs for heat, freshwater and momentum flux calculations, along with three-dimensional coupled ocean-ice-atmosphere models for the Southern Ocean. Most aspects of these investigations were part of the PIPOR Antarctic project for the validation of Synthetic Aperture Radar data (SAR) from the European Remote Sensing Satellite ERS-1.

The main objectives of the passive microwave program were to study the microwave emissivity and polarization of various types of new ice, the effect of a snow cover on the radioactive properties of sea ice and the effect of flooding and the presence of slush at the snow/ice interface. In parallel to the remote sensing activities the temporal and spatial variability of the physical, morphological, chemical, thermal and dielectric properties of snow and sea ice were measured.

The roughness characteristics of sea ice were measured on different scales to construct a data set for validation of sea ice models. Infrared images were obtained using the ship borne HRPT receiving station and a number of radar reflectors were used to study the large scale ice motion. A data set of floe size distribution and lead statistics was acquired using infrared satellite data as well as helicopter borne camera data.

Several sources of remote sensing data were used to derive ice information in support of planning navigation, day to day navigation, and scientific investigations.

Measurement of large-scale sea ice motion

T. Viehoff, S. Rasenat

The ship borne HRPT receiving station was used to collect data from the Advanced Very High Resolution Radiometers (AVHRR) as well as data from the so called TOVS package system (Tiros Operational Vertical Sounder). During the acquisition period the satellite NOAA-9, NOAA-10, NOAA-11, and NOAA-12 were received. About 10 passes per day were obtained and preprocessed. Out of more than 700 passes acquired 170 data sets were selected and stored on tapes for post-processing. The antenna system worked well even under very rough sea state conditions and at very low temperatures (< -30 Cry Because of missing daylight at the times of overpasses only the infrared channels 3, 4 and 5 of the AVHRR were used for sea ice investigations. The data were radiometrically calibrated and geo-coded to allow a direct comparison between different passes. The data will be used to describe the large-scale ice situation under cloud free conditions.

From time series of images the motion of the sea ice was determined using a correlation method similar to the methods used for SAR data analysis. The inertial motion of the ice cover could be measured as well as the mean motion of the ice on time scales of 2-5 days. The results were verified by comparison with the drift information from the ARGOS buoys located in the Weddell Sea. The data from the ARGOS system are included in the HRPT data stream.

The development of ice shelf edge polynyas were monitored for several cases in the Eastern Weddell Sea (0 Meridian to Gould Bay) as well as off the Filchner-Ronne Ice Shelf.

A very interesting result of the first preliminary processing of the data was the discovery of a number of relative high temperature (> -10˚C) patches of 2-20km in diameter within the sea ice cover in the western and southwestern Weddell Sea. These features were monitored over a time period of more then 30 days. Their locations and extents were nearly stationary over the entire period although the surrounding ice cover was moving. The location of at least some of these features seem to be correlated with bathymetric features as the shelf edge and/or submarine mountains. Nevertheless a more detailed analysis will be necessary to describe the physical mechanism responsible for the development of these high temperature patches.

Additionally the data from the ARGOS system were acquired to support the ships Meteorological Office with atmospheric information from the drifting buoys in the Weddell Sea as well as from all other Argos-equipped stations in the vicinity of the Weddell Sea.

All together 41 NOAA AVHRR images were used for near real time ice support for the ship. The information extracted from these data was used to navigate the ship through easier ice conditions near the shelf ice edge as well as through open water leads and/or young ice and refrozen leads in the inner pack ice. The processing of the geo-coded infrared images was performed within half an hour after acquisition of the passes. Additional software was developed to allow the extraction of useful sea ice information by the ship's officers.

Measurement of infrared brightness temperature

R. Brandt, T. Viehoff

A 44-day time series of snow/ice- and water-radiance was measured with a KT-4 radiometer. The data show an instrumental offset of about 4.5 C and an additional air temperature dependence. The data have to be corrected for both effects. The results will be used to calibrate cloud-free data from the NOAA AVHRR infrared channels for atmospheric attenuation effects.

ERS-1 SAR measurements

T. Viehoff

In the period I July - 31 July the German Antarctic Receiving Station has acquired a large number passes of ERS-1 SAR data. From this data set 246 passes had been requested by the AWI remote sensing group. Caused by the heavy ice conditions and logistical constraints only four direct comparison could be made where the ship was in the SAR swath at the time of overpass. Besides of this a number of surface measurements could be performed in a time window ± 1 day of the overpass.

Some of the SAR images were transmitted to the ship by fax, but the relative poor quality of the fax images prevented an analysis of these data. Due to payload faults in the period, 19 July - 24 July, 44 data takes were missing. Fortunately the payload could be reactivated to continue the SAR data acquisition.

The receiving station at O'Higgins was supplied with geo-coding information as for example frame coordinates etc. to allow a preliminary location of the data at the station. The SAR data will be post processed at DLR, Oberpfaffenhofen. The geophysical interpretation of the data with respect to sea ice motion and concentration will be done at the AWI.

Deployment of radar reflectors

W. Dierking, M. Drinkwater

Twelve radar reflectors were deployed in order to supplement ice tracking capabilities from ERS-1 SAR images (Table 5). The first two reflectors were placed on the sea ice to test the reflector design and to check if they could be detected in SAR images. Due to unexpected high drift velocities of the sea ice these two reflectors could not be covered by the SAR swathes.

TABLE 5: Deployment-Positions of the Radar Reflectors

No.	Latitude	Longitude	Date	Time (UTC)
#1	70˚49.95'S	12˚26.15'W	01.07	15:00
#2	71˚37.48'S	16˚33.47'W	05.07	14:00
#3	69˚44.10'S	23˚46.70'W	10.07	06:30
#4	69˚29.90'S	24˚24.60'W	10.07	11:20
#5	69˚41.96'S	26˚15.47'W	10.07	13:00
#6	69˚30.04'S	25˚49.61'W	10.07	14:30
#7	68˚58.70'S	25˚41.30'W	11.07	00:30
#8	68˚16.30'S	24˚59.10'W	11.07	00:30
#9	68˚32.60'S	25˚45.70'W	11.07	00:30
#10	68˚59.90'S	27˚01.60'W	11.07	00:30
#11	68˚29.40˚S	26˚57.00'W	11.07	00:30
#12	68˚14.60˚S	27˚34.60'W	11.07	20:30

The remaining 10 targets were deployed from the ship as well as from helicopter together with a set of 6 meteorological ARGOS drifters (Table 6) in an array of about 200km in diameter. The main drift component during the period from the time of deployment until the end of July was to the northeast which coincides with the results of the large scale ice motion extracted from the AVHRR time series. The radar reflector array was covered several times by a SAR swath. According to a first short analysis done by the O'Higgins operating team the targets could be detected in some of the SAR images. However the detailed analysis of the displacement of the targets will be done as soon as the SAR data are available at AWI.

TABLE 6: Deployment positions of the Argos drifters

No.	Latitude	Longitude	Date	Time (UTC)
9369	69˚44.10'S	23˚46.70'W	10.07	06:30
9368	69˚41.96'S	26˚15.47'W	10.07	13:00
9365	69˚14.50'S	25˚02.30'W	10.07	18:00
9364	68˚43.20'S	26˚18.00'W	11.07	09:00
9367	68˚16.27'S	24˚59.11'W	11.07	14:00
9368	68˚14.60'S	27˚34.60'W	11.07	20:30

Measurement of sea ice concentration and ice types

T. Viehoff, A. Bochert

The sea ice concentration on small scales was estimated during 13 LineScan Camera and/or Video Camera flights. These flights could only be performed during daylight conditions with a sufficient amount of contrast at the sea ice surface. The LineScan data were analyzed onboard the ship to distinguish between at least three classes of ice and open water respectively (Table 7). The main problem of the analysis was to separate between Light Nilas and Grey Ice and to detect refrozen melt ponds at the surface of floes which was observed at the end of the cruise (flight 1-13) after a significant increase of the air temperature caused the snow cover of thinner ice floes to melt.

The preliminary analysis of the data (Table 7) shows the expected result of very high concentrations of white ice in the interior of the Weddell Sea and a more distinctive distribution of the ice classes in the Marginal Ice Zones.

TABLE 7: Measured Sea Ice Type Concentrations (%)

Date	Open Water	Dark Nilas	Light Nilas/Grey Ice		White Ice
15.6.	29.1	8.6	8.1 (L.N.)		54.2
17.6.	0.0	2.9	97.4 (G.I.)		0.0
11.7.	0.2	1.0	2.5 (L.N.)		96.2
14.7.	0.2	2.3	1.0 (L.N.)		96.4

Date	Open Water	Dark Nilas	Light Nilas/Grey Ice		White Ice
19.7.	1.5	1.9	6.5 (L.N)		88.2
26.7.		has to be analyzed			
28.7.	0.3	0.0	14.2 (L.N.)	14.6 (G.I.)	70.2

The Video data were not analyzed on board the ship but were only examined visually to support the LineScan data analysis. Positions are shown in Table 8.

TABLE 8: Positions of Video- and Line-Scan Flights

No.	Latitude	Longitude	Date	Time (UTC)
1	62˚58.47'S	00˚00.42'W	13.06.	11:00
2	64˚31.50'S	00˚00.40'W	14.06.	11:00
3	66˚29.97'S	00˚00.54'W	15.06.	11:00
4.	67˚30.40'S	00˚00.54'W	16.06.	11:00
5	68˚44.20'S	00˚04.00'E	17.06.	11:00
6	71˚37.48'S	16˚33.47'W	05.07.	14:00
7	68˚39.92'S	26˚47.00'W	11.07.	13:00
8	65˚29.61'S	36˚12.52'W	14.07.	15:00
9	63˚26.07'S	43˚31.03'W	19.07.	16:00
10	62˚05.65'S	43˚48.46'W	21.07.	16:00
11	62˚00.41'S	43˚55.69'W	22.07.	13:00
12	60˚13.51'S	47˚09.28'W	26.07.	16:00
13	59˚50.18'S	50˚33.77'W	28.07.	15:00

Measurement of sea ice surface topography

W. Dierking, S. Rasenat

A laser profiler mounted on a helicopter was used to measure the surface topography of sea ice along the cruise leg. The profiles were collected at a sampling rate of 100Hz. Depending on flight conditions, the horizontal resolution varied between 15 and 25cm. The effective vertical resolution was 2cm. At the nominal flight altitude of 30m the laser footprint on ground was about 8cm in diameter. Altogether 17 laser flights were performed amounting to a total profile length of 428nm.

Between 26 and 29 June, eight 10nm profiles were measured near Atka Bay. During this period a nearly stationary area of rafted and ridged consolidated ice was separated from drifting pack ice by a shear line approximately located 10nm off the shelf edge. Four of the laser profiles were flown parallel to the shear line (two on either side) at a distance of 2nm and 4nm, respectively. The other four profiles were crossing the shear zone. The height and spacing distributions of ice roughness features were investigated separately for the stationary ice area between shear line and shelf edge and the drifting pack ice on the other side of the shear line. The preliminary results show a nearly exponential decrease of ridge frequency as a function of ridge height in the drifting pack ice, whereas the

histograms of the stationary ice area reveal a Rayleigh-shaped distribution function. The mean ridge height, however, is the same on both sides. The mean ridge spacing increases with distance off the shear line. In the vicinity of the shear line, the average values are 14m for the stationary ice and 19m for the drifting ice. At a distance of 4nm from the shear line the values are 25m and 40m respectively.

The data sets from 13 - 14 July were analyzed as an example of the topographic characteristics in an area of divergent ice drift in the center of the Weddell Sea. Both the height and spacing distributions show an exponentially decreasing number of ridges as a function of ridge height and spacing, respectively. The mean ridge heights are 1.4m and 1.3m, and the mean ridge spacing are 69m and 62m. Floes of un-deformed ice as large as 300 to 700m were observed. A sufficient number of open water leads and areas of thin ice were crossed during the flights to enable an estimate of the freeboard. The mean freeboard, including the snow cover, was 19 and 22cm, respectively.

Test of NOAA-APT/OKEAN-RAR data acquisition system

W. Dierking, T. Viehoff

A low cost PC-based APT receiving station designed by the DLR Satellite Receiving Station at Neustrelitz for acquisition of OKEAN RAR data as well as for NOAA APT data was tested. Unfortunately the acquisition of the OKEAN-4 data could not be carried out because of a delay of the satellite launch. The NOAA-APT data were received and processed successfully. This was done parallel to the data acquisition by the ship's Met Office.

International Space Year (ISY) activities

C. Garrity, A. Bochert

As part of the International Space Year (ISY), ice maps were transmitted by INMARSAT facsimile to FS Polarstern during the expedition. The ice information originated from two sources: Defense Meteorological Satellite Program (Special Sensor Microwave/Imager (SSM/I)) and the European Space Agency Remote Sensing Satellite (ERS-1) (Synthetic Aperture Radar (SAR)). The SSM/I brightness temperatures (Tg) were obtained directly from the Fleet Numerical Oceanographic Center in Monterey, USA to the Alfred Wegener Institute (AWI) using a computer modem. The data transfer to AWI was funded by ISY. R. O. Ramseier, who was on secondment from AES for one year, processed Tg's using the AES algorithm, providing the ship with ice maps of total, thin and old ice concentrations within 4-6 hours after the satellite overpass. These maps proved to be very useful for planning purposes, especially in order to avoid high concentrations of old ice. The SAR data was received directly from the ERS-1 satellite by K. W. Asmus and K. Strubing, at a German receiving station located at O'Higgins, at the tip of the Antarctic peninsula. The reception of data was successful, however, the SAR images received on the ship were poor quality. Only sketches showing the interpretation of the original images were of interest. The captain did not use the ERS-1 SAR derived ice information for navigation of the ship. The SSM/I products combined with images received directly on the ship from the NOAA satellites (Advanced Very High Resolution Radiometer (AVHRR)

images) proved to be a good combination to aid navigation of a ship through the ice. However, cloud free conditions were required for the AVHRR images to be useful for ice information.

It is the ultimate aim to combine ice information obtained from the 30m resolution SAR with the 25km resolution SSM/I maps. However, further understanding of back-scatter from snow and ice is required before features on a SAR image can be interpreted. It is for this reason that measurements of the snow and snow/ice interface, ship-based Tg's and quantitative ice concentrations obtained from a helicopter in an area of the satellite footprints were completed.

C. Hydrographic Measurements

The objectives of the oceanographic program were:

- Calculation of volume, heat, and salinity fluxes between Atlantic and Indian ocean and within the regime of the Weddell Gyre.
- Calculation of the geostrophic shear in the different current bands of the Antarctic Circumpolar Current (ACC) and the Coastal Current (CC) along the eastern and western Antarctic shelf.
- Definition of water mass characteristics within the circumpolar belt and the Weddell Sea, including the variability of natural and anthropogenic tracers.
- Detection of the variability of the ACC with an ADCP along the Greenwich Meridian and across the Drake Passage.
- Description of the variability of the ACC across the Drake Passage with temperature profiles from XBTs and comparison of seasonal changes with other XBT cruises.
- Measurement of the turbulent heat- and momentum fluxes in the oceanic boundary layer below the sea ice during winter conditions.

WOCE one-time section A12:

Oceanographic work started on May 22 with a test station in 2100m water depth at the shelf break southwest of Cape Town. After steaming back to the beginning of the first transect the routine CTD work began with a normal distance of 40nm between stations, decreasing to 15nm at the slopes of the continental shelf breaks. Additionally, en route registrations of the ADCP and thermosalinograph were done. The ADCP data set had to be carefully analyzed at home whereas the surface values of temperature and salinity (at 8 m depth) provided a useful tool in detecting frontal systems during the cruise. The position of the oceanic fronts, the Subtropical Front (STF), the Subantarctic Front (SAF), the Polar Front (PF), and the Continental Water Boundary (CWB) were dominated by large horizontal gradients in T and S that amount to the following winter values:

	∆-Temp (C)	**∆-Salinity (PSU)**
STF:	7.0	1.0
SAF:	3.5	0.4
PF:	1.5	0.2

Except for the Polar Front these gradients were higher than in the summer season (Bathmann U., et al, 1992). In ice covered regions the thermosalinograph did not work because of freezing within the pump system. Therefore, values for the gradient at the CWB could not be detected. The oceanographic fronts and the main water mass characteristics in the Atlantic sector of the Southern Ocean along the Greenwich Meridian. The hydrographic parameters of potential temperature (E)), salinity (S), phosphate (PO_4), and silicate (SiO_3) are chosen as examples, which can be used to identify the different water masses in this part of the ocean. The vertical extent of these water masses can also clearly be seen in CTD profiles. North of 56˚S, which is the southernmost extension of the mid ocean ridge in this area, the different water masses could most easily be traced by salinity, whereas in the Weddell Gyre the temperature is the better parameter to identify specific water types on a large scale. Looking from north to south the upper water column (0-1000m) is dominated by the surface waters of the subtropical gyre (north of the STF) and Subantarctic Surface Water (SASW) between STF and SAF that are high in salinity and temperature but poor in oxygen and nutrients. The belt of strong winds and high precipitation between Subantarctic and Polar Front is the source region of the Antarctic Intermediate Water (AAIW) which is characterized by low salinity and high oxygen values. This tongue sinks towards the north and spreads into the southern Atlantic at a depth range of 500- 1200m. In the upper 200m south of the PF the water is cold, fresh, rich in oxygen and high in nutrients as compared to the SASW. It is composed of Antarctic Surface Water (AASW) and/or Winter Water (WW) which is cooled to the freezing point. Near the continent the pycnocline isolating the convective layer from the Warm Deep Water (WDW) underneath deepens towards the shelf down to 600m. At the shelf break less saline waters of the Coastal Current (CC) regime appear which have lower oxygen but higher nutrient concentrations as the surrounding water masses. Depending on ice conditions and incoming solar radiation these values can change rapidly.

The deep ocean (>1000m) is dominated by the Circumpolar Deep Water (CDW) which is the most extensive water mass with a thickness of more than 3000m. It can be divided into the Upper CDW (UCDW) with its source in the Indian and Pacific oceans which provide its high nutrient and low oxygen values, and the Lower CDW (LCDW), which is fed in the North Atlantic Deep Water (NADW) moving southward with a maximum in salinity and oxygen and a minimum in nutrients. Entering the ACC the axis of both parts is inclined upward to the south compensating the northward flowing Antarctic Bottom Water (AABW) which spreads as a tongue of cold, fresh water with high oxygen and nutrient values into the great ocean basins. It fills the lowest 500m above the bottom north of the mid-ocean ridge system at 56˚S. In the deep Weddell basin the oceanic structure looks quite different because of the large vertical extension of the AABW which is always detectable at depths greater than 2000m with a doming in the gyre centre up to 1200m. It has the largest silicate values of the world ocean with more than 130.0mmol/l. Near the bottom at depths of more than 4500m the influence of the Weddell Sea Bottom Water (WSBW) can be seen from the decreasing temperatures, salinities, and silicate values, and increasing oxygen. Pure WSBW was not detected on this transect.

Between the WW at the surface and the AABW the warm and salty WDW is trapped south of the ACC. It has its origin in the LCDW that circles the cyclonic Weddell Gyre at its eastern end and enters the southern part of the Weddell Gyre above 1500m (Whitworth and Nowlin, 1987). The heat content of this water mass is used to balance the overall heat loss to the atmosphere south of the Polar Front. The fronts on the Greenwich Meridian are relatively narrow and their signatures are detectable down to greater water depths. Only the Polar Front seems to be smeared out over a larger distance. At the Subantarctic Front for example the sharp horizontal gradients extend from the surface to the bottom (more than 3500m). South of the Polar Front near Station 577 the transition from the Antarctic Circumpolar Current to the current regime of the Weddell Gyre is also marked by an increase of the shoaling of isolines. Calculated baroclinic geostrophic velocities from 50dbar relative to the bottom show the broad eastward flowing circumpolar current with three bands of strong geostrophic velocities up to 18cm/s at the surface and of more than 3cm/s at 2000m depth. The bands are located between SAF and PF. The complicated flow structure north of the SAF results from the influence of the Agulhas retroflection, the South Atlantic Current (SAC); and the northern limb of the ACC which all form a region of very high eddy activity due to strong horizontal current shear and highly variable water mass composition.

Weddell Gyre (WOCE repeat section SR04)

Because of the severe ice conditions the cruise track in the Weddell Basin had to be modified to focus on two hydrographic sections, one starting at the centre of the gyre (station 623 at 66˚S 33˚5'W) running northwest to the South Orkney shelf, and the other closing the gap between the shallow (<500m) areas west of South Orkney and east of Clarence Island. As known from previous cruises (Augstein et al., 1991) doming of isolines in the middle of the cyclonic Weddell Gyre (stations 626-629) dominate the structure of all oceanic parameters. The downward slope near the shelf break is not as steep as on the eastern boundary but is clearly visible. The temperature maximum of the WDW (Q > 0.4˚C) is divided into two cores where the western cell has its centre position at 44˚W. This was already sampled in late winter 1989 and summer 1990 by other POLARSTERN expeditions (WWGS'89, SWGS'90).

In the deep ocean Weddell Sea Bottom Water (WSBW) was found between station 624 and 633. It differs from the water mass above (AABW) through lower temperature (Q < -0.8˚C), lower salinity (s < 34.65), lower nutrient values (for example silicate less than 125.0RM), and higher oxygen values (Ox > 5.7ml/l).

The most undiluted WSBW is located of a water depth of 2700-4000m at the continental slope as a 100 - 300m thick lens. A second core fills the flat bottom of the deep Weddell basin at water depths of more than 4500 m. Its thickness is also less than 300m. This splitting into two branches suggests that different sources of WSBW exist, some of which are known as the Filchner trench and the wide shelf areas along the Antarctic Peninsula. Careful interpretation of the hydrographic parameters together with the analysis of tracer measurements from the water samples should give more information on the pathways and possible source areas.

The comparison with previous cruises further south (WWGS'89, SWGS'90, and with the American/Russian drift station ISW'92) will improve our understanding of the formation mechanisms of WSBW. The northernmost section between the shelves of Clarence Island and South Orkney was taken to investigate the possible inflow and outflow to/from the Weddell Sea. Due to the limited water depth (maximum 2400m) no WSBW is leaving the basin through this gap. In the depth range 200 to 1500m an outflow of WDW out of the Weddell Sea occurs at the eastern flank of this section. High temperatures and salinities, and low oxygen values indicate that this water originates from the western core of the WDW which is divided by the wide and shallow South Orkney shelf.

C.1 Instrumentation

M. Schröder, A. Wisotzki, N. Brunken, I. Hansen, P. Heil, M. Kreyscher, S. Moschner, N. Steiner, U. Sterr, K. U. Richter, H. Diedrich

The instrumentation used included: CTD (NB MkIIIB) General Oceanic Rosette (24 x 12 1) Salinometer (Autosal) Autoanalyzer (Technicon System II). During the long ice station: CTD plus three component acoustic current meter (Simtronix UCM-40 Mk II) were used.

C.2 CTD measurements

The CTD-measurements were carried out with two NB Mark IIIB sondes connected to a General Oceanics rosette water sampler with 24 12-liter bottles. Due to damaged sensors the CTD-sonde had to be exchanged after station 623.

The quality of the CTD-data relies on the laboratory calibrations of the temperature and pressure sensors made before the cruise at the Scripps Institution of Oceanography for each sonde. The performance of the instruments during the cruise was controlled by use of SIS digital thermometers and pressure meters. The pre-cruise temperature and pressure calibration values were applied to the measurements on board (see enclosed calibration table). The conductivity values of the CTD were corrected by means of salinity measurements from the rosette water samples. Differences between bottle samples and CTD readings for each profile were calculated. The stratification of the water column near the surface caused higher scattering of these differences and so only values in levels deeper than 500 m are used for correction. The preliminary data presented in this report are corrected by a constant offset of 0.042 (station 535-623) and 0.062 (station 624-649). The accuracy of the preliminary data was estimated to 3m°K in temperature, 3dbar in pressure and 0.003 PSU in salinity.

C.3 Water sample salinities

The salinity of the water samples was determined with a Guildline Autosal 8400 A salinometer in reference to IAPSO Standard Seawater (batch number P114). The salinities are given in PSU and calculated by use of the UNESCO Practical Salinity Scale (PSS78).

C.4 Water sample oxygen measurements

The concentration of dissolved oxygen was measured by means of a computer controlled SIS Winkler-titrator from 1912 samples taken at 98 stations. In addition 10 % of all samples were measured as double samples from the same bottle. The standard error of all double samples ranged between 0.05 and 0.1µM with a standard deviation from 0.2 to 0.5µM corresponding to an overall precision of 0.10 to 0.15 %.

C.5 Dissolved nutrients

Water samples were collected with the oceanographic rosette sampler and analyzed on a Technicon Autoanalyzer II system. Nitrate was determined as nitrite after reduction with cadmium and reaction with sulfanilamide and N-(1naphtyl)-ethylendiamindihydrochlorid as red colored azoyde at 20nm. Ammonium was measured as blue colored indophenole at 30nm after the reaction with phenolate and hypochlorite under alkaline conditions (Berthelot reaction). For the determination of silicate and phosphate the compounds react with ammonium molybdate by forming a blue molybdate-complex that was measured at 60nm respectively at 880nm.

All nutrient samples were analyzed in duplicate; precision was estimated at 0.1µmol L-1 for nitrate, 0.3µmol L-1 for silicate and 0.01µmol L-1 for phosphate. The accuracy was set by running four standards at the beginning and two standards at the end of each run.

C.6 Chlorofluorocarbons

K. Bulsiewicz, W. Plep, H. Rose, and J. Sultenfuss

Along the two hydrographic WOCE sections A12 and SR04 the CFMs Freon-11 and Freon-12 were measured using an automated version of the Bullister and Weiss technique. The data sets provide important information about circulation and renewal pathways for all relevant subsurface water masses.

Water samples were taken in the usual way using glass syringes. A total of 86 tracer stations were occupied. 1600 water samples for the fluorocarbons F-11 and F-12 were analyzed during the cruise.

On the WOCE section A12 (Cape Town-Antarctica) CFM-free deep water was found at greater depths up to 43 S. With this data and a special calibration cast that was made into supposedly CFC free water in the Drake Passage, the overall blank can be checked. This is important for the precision of the data, since the measurement of water samples require an additional correction for the blank. The measurements of these waters showed consistently low values of 0.01-0.02pmol/kg for both CFMs, which is a good value in comparison of the measured range of these compounds (approximately 0.1-8pmol/kg for F-11 and 0.1-3.3pmol/kg for F-12).

Measurements of near surface waters under the ice, showed that the dissolved CFC concentrations are only about 70% of those predicted for equilibrium with the atmosphere.

The under-saturation reflects the restriction of the air-sea exchange due to the sea ice cover.

Measurements at stations 623-629 indicate unknown water mass at a depth of 2200m. This could be a sign of regional convection processes. At station 631 the data indicate the presence of high CFC waters (F-11 concentration > 1.8pmol/kg) at a depth ranging between the bottom and about 3850m. This is a clear indication of Antarctic Bottom Water.

C.7 Helium/tritium

K. Bulsiewicz, W. Plep, H. Rose, and J. Sultenfuss

Water samples were taken in the usual way using copper tubes (Helium), glass bottles (Tritium). For the new technical system to extract helium directly on ship, water samples were taken in 50ml glass pipettes. Samples were collected for analysis ashore from 30 stations for tritium (600 water samples) and 47 stations for helium (880 water samples, 410 with the extraction method).

C.8 The carbon dioxide system in Antarctic waters

J. M. J. Hoppema and J. J. M. Belgers

Of all gases causing the man-made greenhouse effect carbon dioxide (CO_2) is the most important one. A significant part of the excess CO_2 which is brought into the atmosphere is thought to be taken up by the oceans. However, the spatial and temporal extent of the uptake is far from manifest. To gain this important knowledge the data set of oceanic CO_2 measurements has to be enlarged significantly. Data collected during the cruise constitute an important supplement to the worldwide oceanic data set of CO_2, because winter data of the Weddell Sea are scarce. Particular objectives were to investigate the following features:

1. Contrary to the temperate and tropical oceans the water column in the Antarctic Ocean has a low vertical stability, which could give rise to important vertical fluxes of CO_2. This condition is most pronounced in winter.
2. The total CO_2 (TCO_2) content and the alkalinity of a water mass are unique properties, dependent on its history. This renders TCO_2 and alkalinity potential tracers.
3. From TCO_2 and alkalinity the partial pressure of CO_2 (pCO_2) can be calculated. With this property the exchange of CO_2 between ocean and atmosphere can be determined. In the ice-covered areas pCO_2 can tell something about the CO_2 content the water has when it leaves the surface, and thus how much (excess) CO_2 is brought down to deeper waters.

Measurements:

CO_2 in seawater is involved in a series of chemical reactions leading to ionic species. Therefore, to measure CO_2 in seawater one actually needs to determine the CO_2 system.

It turns out that by measuring 2 parameters of the system one is able to calculate the whole system. During the cruise TCO_2 and total alkalinity were measured. TCO_2 was measured with a standard coulometric method. Alkalinity was measured by means of a potentiometric acid titration, which consisted of first adding an excess quantity of hydrochloric acid beyond the alkalinity endpoint and then recording the readings of the pH electrode after some small additions of acid. The endpoint was determined with a Gran method.

Water was taken from the Rosette at almost all CTD stations in Antarctic waters during the cruise. For TCO_2 24 samples were normally taken through the whole water column, with samples in the surface layer more closely spaced; at the shallower stations the number of samples was less. Water for alkalinity determination was sampled through the whole water column only at selected stations, while at the other stations only the surface water layer was analyzed. In between stations some continuous on line measurements for TCO_2 were conducted.

Fig. 2.1 - 12 shows three depth profiles for TCO_2, two within the Weddell Sea and the other one at the Subantarctic Front (SAF) in the Atlantic Ocean. Data on the alkalinity will become available later. All profiles show the feature usually observed in TCO_2 profiles that there is a surface depletion compared to the deep water. However, the extent of depletion was different, in the centre of the gyre it was much less than at the SAF. This is a combined effect of different surface water temperatures and biological activity, which both are higher at the SAF. Also in the deep water there were striking differences between the profiles. In the Weddell Sea a single TCO_2 maximum was observed at about 700-900m depth, whereas at the SAF the maximum lies at about 1300m. Furthermore, at the SAF TCO_2 increases again towards the bottom. Here we see the interplay of different water masses of different origin. Between the two Weddell Sea stations there were also some slight differences. The TCO_2 maximum at station 633 was more pronounced than at station 619, while the TCO_2 concentration at the maximum is about equal. Surface TCO_2 concentration in the centre of the gyre was higher. This suggests that the water in the centre of the gyre was in contact with the atmosphere more recently than the water at station 633. A more detailed analysis of the data will include all stations and will also relate to other quantities measured during the cruise.

C.9 Neon

not measured

D. Acknowledgements

E. References

Augstein, E., N. Bagriantsev, H. W. Schenke (eds.), 1991: The Expedition ANTARKTIS VIII/1-2, 1989, with the Winter Weddell Gyre Study of the Research Vessels Polarstern and "AKADEMIK FEDOROV". Ber. Polarforsch. 84: 1-134.

Bathmann, U., M. Schulz-Baldes, E. Fahrbach, V. Smetacek, H.-W. Hubberten (eds.), 1992: The Expedition ANTARKTIS IX/1-4 of the Research Vessel Polarstern in 1990/91. Ber. Polarforsch. 100: 1-403.

Unesco, 1983. International Oceanographic tables. Unesco Technical Papers in Marine Science, No. 44.

Unesco, 1991. Processing of Oceanographic Station Data. Unesco memograph By JPOTS editorial panel.

Whitworth, T. III, W. D. Nowlin, Jr., 1987: Water Masses and Currents of the Southern Ocean at the Greenwich Meridian. J. Geophys. Res., 9 2, 6462-6476.

F. WHPO Summary

Several data files are associated with this report. They are the ANTX4.sum, ANTX4.hyd, ANTX4.csl and .wct files. The ANTX4.sum file contains a summary of the location, time, type of parameters sampled, and other pertient information regarding each hydrographic station. The ANTX4.hyd file contains the bottle data. The .wct files are the ctd data for each station. The .wct files are zipped into one file called ANTX4.wct.zip. The ANTX4.csl file is a listing of ctd and calculated values at standard levels.

The following is a description of how the standard levels and calculated values were derived for the ANTX4.csl file:

Salinity, Temperature and Pressure:
These three values were smoothed from the individual CTD files over the N uniformly increasing pressure levels using the following binomial filter-

$$t(j) = 0.25ti(j-1) + 0.5ti(j) + 0.25ti(j+1) \quad j=2....N-1$$

When a pressure level is represented in the .csl file that is not contained within the ctd values, the value was linearly interpolated to the desired level after applying the binomial filtering.

Sigma-theta(SIG-TH:KG/M3), Sigma-2 (SIG-2: KG/M3), and Sigma-4(SIG-4:KG/M3): These values are calculated using the practical salinity scale (PSS-78) and the international equation of state for seawater (EOS-80) as described in the Unesco publication 44 at reference pressures of the surface for SIG-TH; 2000dbars for Sigma-2; and 4000dbars for Sigma-4.

Gradient Potential Temperature (GRD-PT: C/DB 10-3) is calculated as the least squares slope between two levels, where the standard level is the center of the interval. The interval being the smallest of the two differences between the standard level and the two closest values. The slope is first determined using CTD temperature and then the adiabatic lapse rate is subtracted to obtain the gradient potential temperature. Equations and Fortran routines are described in Unesco publication, Processing of Oceanographic Station Data, 1991.

Gradient Salinity (GRD-S: 1/DB 10-3) is calculated as the least squares slope between two levels, where the standard level is the center of the standard level and the two closes values. Equations and Fortran routines are described in Unesco publication, Processing of Oceanographic Station Data, 1991.

Potential Vorticity (POT-V: 1/ms 10-11) is calculated as the vertical component ignoring contributions due to relative vorticity, i.e. pv=fN2/g, where f is the coriolius parameter, N is the bouyancy frequency (data expressed as radius/sec), and g is the local acceleration of gravity.

Bouyancy Frequency (B-V: cph) is calculated using the adiabatic leveling method, Fofonoff (1985) and Millard, Owens and Fofonoff (1990). Equations and Fortran routines are described in Unesco publication 44.

Potential Energy (PE: J/M2: 10-5) and Dynamic Height (DYN-HT:M) are calculated by integrating from 0 to the level of interest.Equations and fortran routines are described in Unesco publication, Processing of Oceanographic Station Data, 1991.

Neutral Density (GAMMA-N: KG/M3) is calculated with the program GAMMA-N (Jackett and McDougall) version 1.3 Nov. 94.

G. Data quality Evaluation

HELIUM - NEON ISOTOPE DATA DOCUMENTATION

EXPOCODE 06QANTX/4 WHP_ID SR4
The data was aquired by
Prof. Dr. Wolfgang Roether
Tracer-Ozeanographie
FB1
Universitaet Bremen
PO. Box. 330 440
28334 Bremen
Tel.: 0421/218-3511 / 4221
Fax: 0421/218-7018
email: wroether@physik.uni.bremen.de

responsible for measurement and data processing:

Christine Rueth
Tel: 0421/210-4317
email: crueth@pacific.physik.uni-bremen.de

Two different sets of samples were taken:

1. Most samples were taken in the usual manner with pinched- off copper tubes. After the gas extraktion in Bremen they were measured in the Laboratory with a dedicated Helium - Neon Isotope Mass Spectrometer.

2 Another set was sampled into glas-pipettes and extracted at sea. The glas ampulles with the extracted gas were then transported back to Bremen for measurement.

All samples were calibrated using an air standard (regular air) in the Bremen laboratory. The samples of the whole cruise were measured using the same air standard.

The samples are corrected for tritium decay during storage time, using the tritium concentration measured in the tritium samples that were taken from the Bremen group as well.

Data quality:
The realtive errors for the measured properties can be given as

1. Copper-tube set:

   Helium: 0.36 %
   Neon: 0.49 %
   He3/He4: 0.31 %

2. Due to different processes the errors of the sea-extracted samples are about 0.1 % enhanced

   Helium: 0.37 %
   Neon: 0.50 %
   He3/He4: 0.32 %

DQE of CTD data for the ANT-10th cruise of the r/v "Polarstern", WOCE section A12 – SR04 in the South Atlantic

Eugene Morozov

Data quality of 2-db CTD temperature and salinity profiles and reference rosette samples with oxygen measurements were examined. Vertical distributions and theta-salinity curves were compared for individual stations using the data of up and down CTD casts and rosette probes. Data of several neighboring stations were compared.
Listing of results from the comparison of salinity data. Only those stations are listed which have data remarks.

Station	Pressure	Remarks
551	69 db	Low SALNTY (34.405), flag 3
	220 db	Low SALNTY (34.493), flag 3
	504 db	Low SALNTY (34.219), flag 3
563	220 db	High SALNTY (34.488), flag 4
	399 db	Low SALNTY (34.273), flag 3
564	300 db	Low SALNTY (34.361), flag 4
593		Low CTDSAL calibration almost for the entire station. CTDSALes are by 0.002 – 0.003 less than bottle measurements.
595	2401 db	High SALNTY (34.666), flag 3
597	4678 db	High SALNTY (34.653). flag 3
601		CTDSAL calibration is lower than norm. CTDSALes are less than bottle SALNTYes by 0.02 – 0.03 below 2000 db.
602		CTDSAL calibration is higher than norm. CTDSALes are greater than bottle SALNTYes by 0.02 – 0.03 below 700 db. Bottle SALNTY measurements indicate a slight decrease of salinity between stations 601 and 602 below 1000 db, but CTDSALes do not.
603		CTDSAL calibration is higher than norm. CTDSALes are greater than bottle SALNTYes by 0.04 – 0.07 for the entire depth.
610	A shallow station with many bad bottle SALNTY measurements.	

pressure	upcast CTDSAL	SALNTY	downcast CTDSAL	SALNTY flag
49	34.208	34.221	34.208	4
100	34.210	34.216	34.210	4
149	34.210	34.218	34.210	4
249	34.211	34.198	34.211	4
300	34.211	34.202	34.211	4
397	34.223	34.233	34.223	4

618	449 db	Low SALNTY (34.682), flag 4
624	2599 db	Low SALNTY (34.654), flag 3 (bottle 9)
625	4199 db	Low SALNTY (34.637), flag 4
626	2599 db	Low SALNTY (34.655), flag 3 and again bottle 9 at the

		same level
633	CTDSAL calibration is higher than norm below 1000 db.	
639	CTDSAL calibration is higher than norm below 1000 db.	
642	796 db	Low SALNTY (34.628), flag 3

It is a pity that there were no CTDOXY measurements in the cruise. It is much more difficult to make data quality evaluation without continuous measurements. Anyhow I find that some of the bottle OXYGEN fall off the distribution curves:

Station	Pressure	Remarks
539	2399 db	High OXYGEN (247.2), flag 3
540	750 db	Low OXYGEN (184.9), flag 3
541	600 db	Low OXYGEN (193.5), flag 3
552	698 db	Low OXYGEN (226.5), flag 3
556	3399 db	High OXYGEN (234.8), flag 3
	4199 db	High OXYGEN (229.7), flag 3
574	2496 db	High OXYGEN (218.0), flag 3
585	3500 db	Low OXYGEN (235.3), flag 3
591	1200 db	High OXYGEN (218.0), flag 3

INPUT FILE: antx4.EGM
THE DATE TODAY IS: 12-MAY-95

STN NBR	CAST NO	SAMP NO	CTD PRS	CTD SAL	CTD OXY	SALNTY	OXYGEN	QUALT 1	QUALT 2
539	1	3	2399.0				247.2	~~~2	~~~3
540	1	14	750.8				184.9	~~~2	~~~3
541	1	13	600.7				193.5	~~~2	~~~3
551	1	23	69.3			34.4052		~~2~	~~3~
551	1	21	220.5			34.4932		~~2~	~~3~
551	1	17	504.7			34.2192		~~2~	~~3~
552	1	15	698.5				226.5	~~~2	~~~3
556	1	6	3399.0				234.8	~~~2	~~~3
556	1	4	4199.8				229.7	~~~2	~~~3
563	1	19	399.3			34.2736		~~2~	~~3~
574	1	1	2496.5				218.0	~~~2	~~~3
585	1	7	3500.4				235.3	~~~2	~~~3
591	2	13	1200.2				201.9	~~~2	~~~3
595	3	7	2401.1			34.6662		~~2~	~~3~
597	1	2	4678.7			34.6531		~~2~	~~3~
610	1	8	49.2			34.2212		~~2~	~~4~
610	1	7	100.4			34.2161		~~2~	~~4~
610	1	6	149.9			34.2182		~~2~	~~4~
610	1	4	249.4			34.1982		~~3~	~~4~
610	1	3	300.0			34.2020		~~2~	~~4~
610	1	1	397.5			34.2332		~~2~	~~4~
618	3	2	449.8			34.6820		~~2~	~~4~
624	1	8	2999.5			34.6548		~~2~	~~3~
625	3	5	4199.7			34.6449		~~2~	~~4~
626	3	9	2599.3			34.6549		~~2~	~~3~
642	1	7	796.4			34.6282		~~2~	~~3~

A12 preliminary (06AQANTX-4)

Panel A: Salinity [PSS 78]
Panel B: pot. Temperature [deg C ITS 68]
Panel C: Oxygen [umol/kg]
Panel D: Silicate [umol/kg]
Panel E: Nitrate [umol/kg]
Panel F: Phosphate [umol/kg]

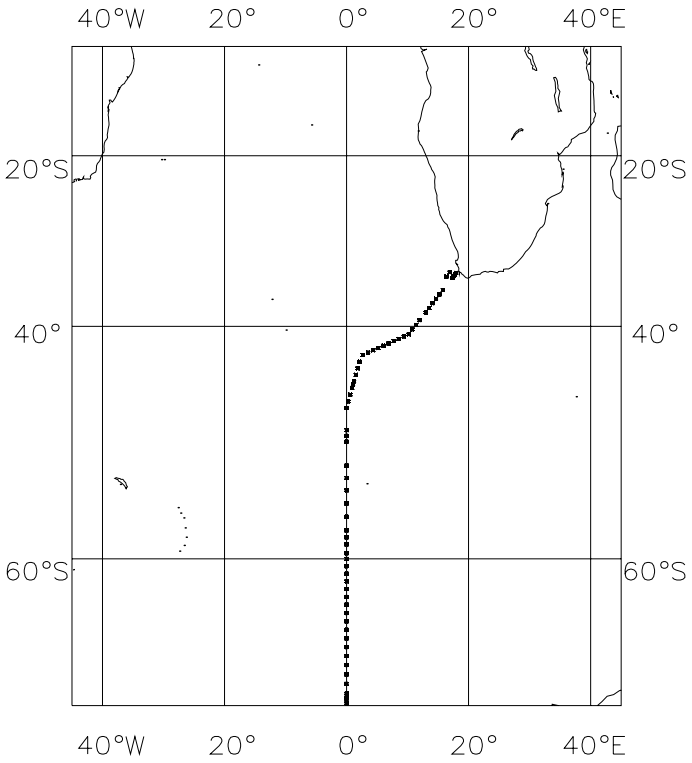

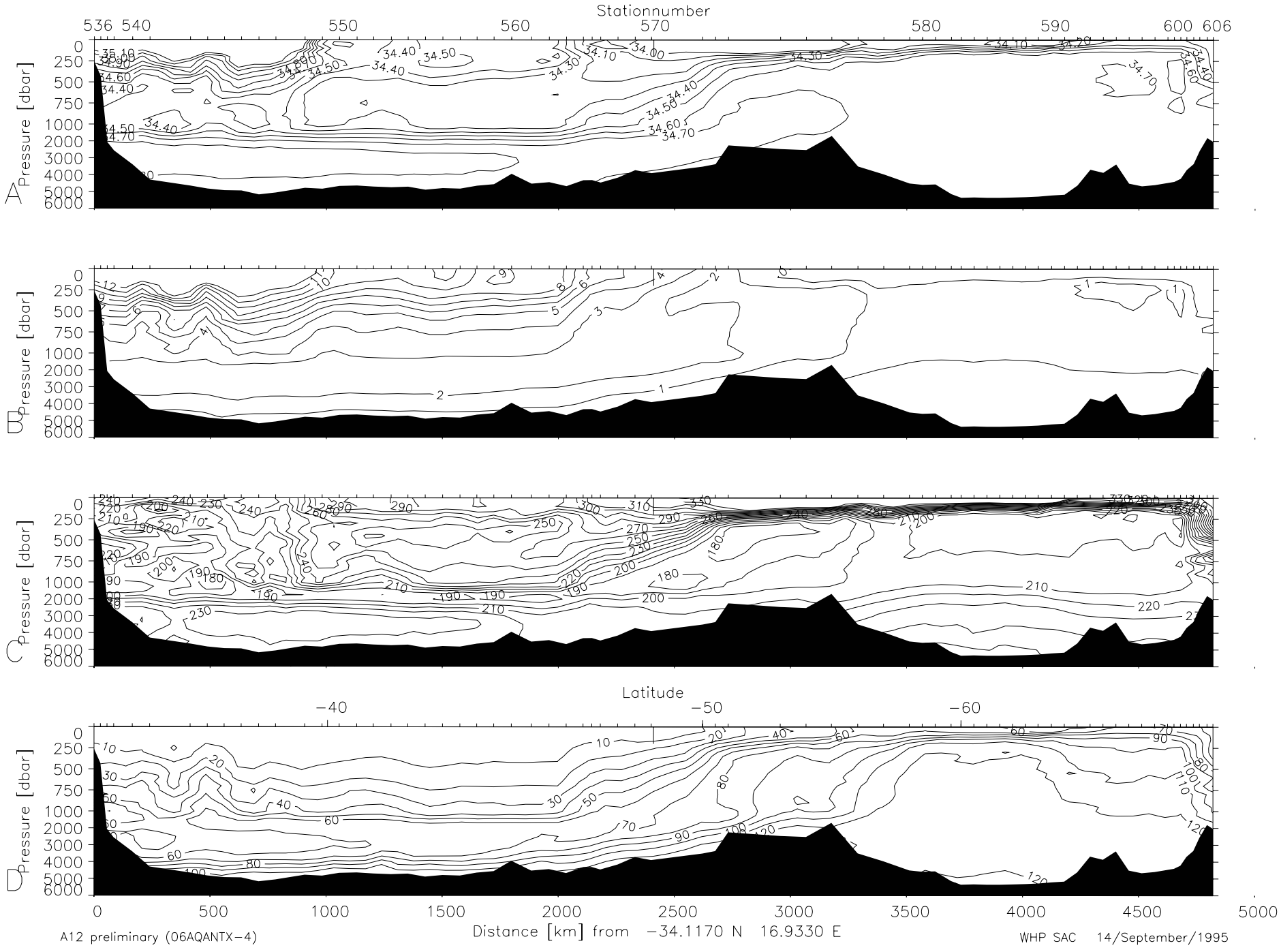
Stationnumber
536 540 550 560 570 580 590 600 606
A
B
C
D
Pressure [dbar]
0 250 500 750 1000 2000 3000 4000 5000 6000
Latitude
−40 −50 −60
0 500 1000 1500 2000 2500 3000 3500 4000 4500 5000
Distance [km] from −34.1170 N 16.9330 E
A12 preliminary (06AQANTX−4)
WHP SAC 14/September/1995

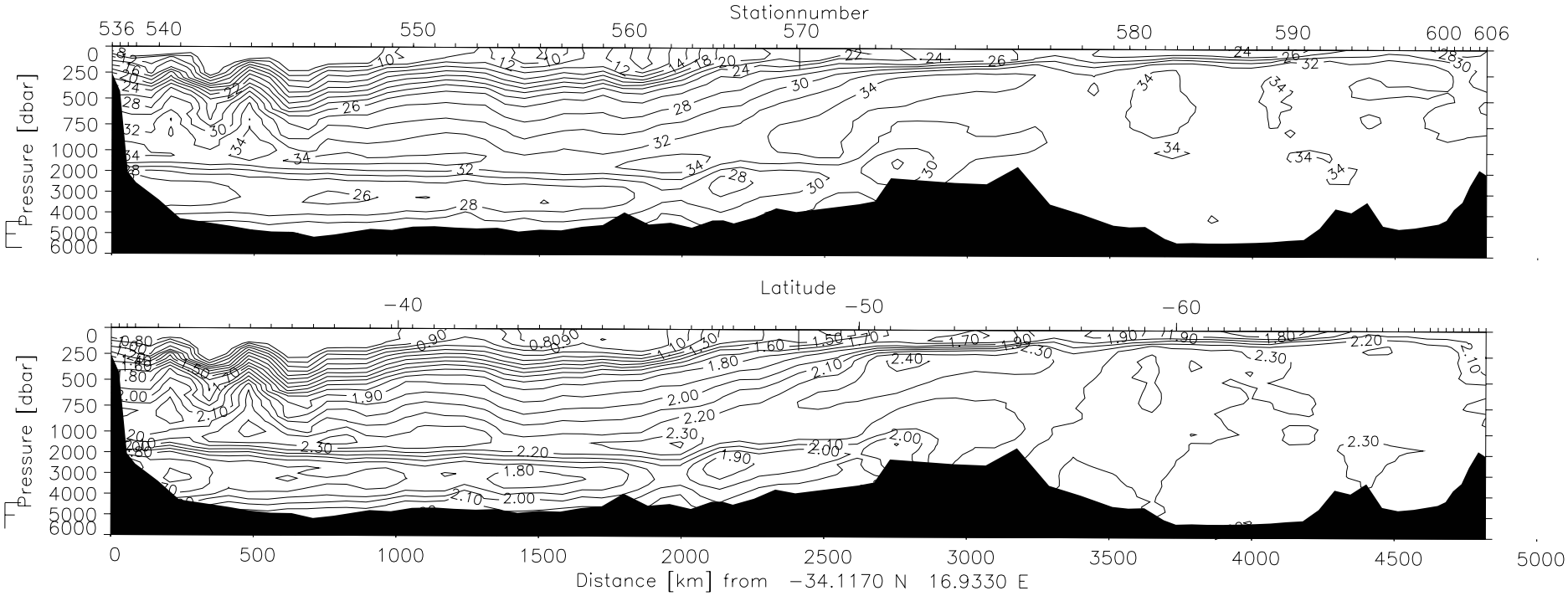
Stationnumber
536 540 550 560 570 580 590 600 606
Pressure [dbar]
0 250 500 750 1000 2000 3000 4000 5000 6000
Latitude
−40 −50 −60
0 500 1000 1500 2000 2500 3000 3500 4000 4500 5000
Distance [km] from −34.1170 N 16.9330 E

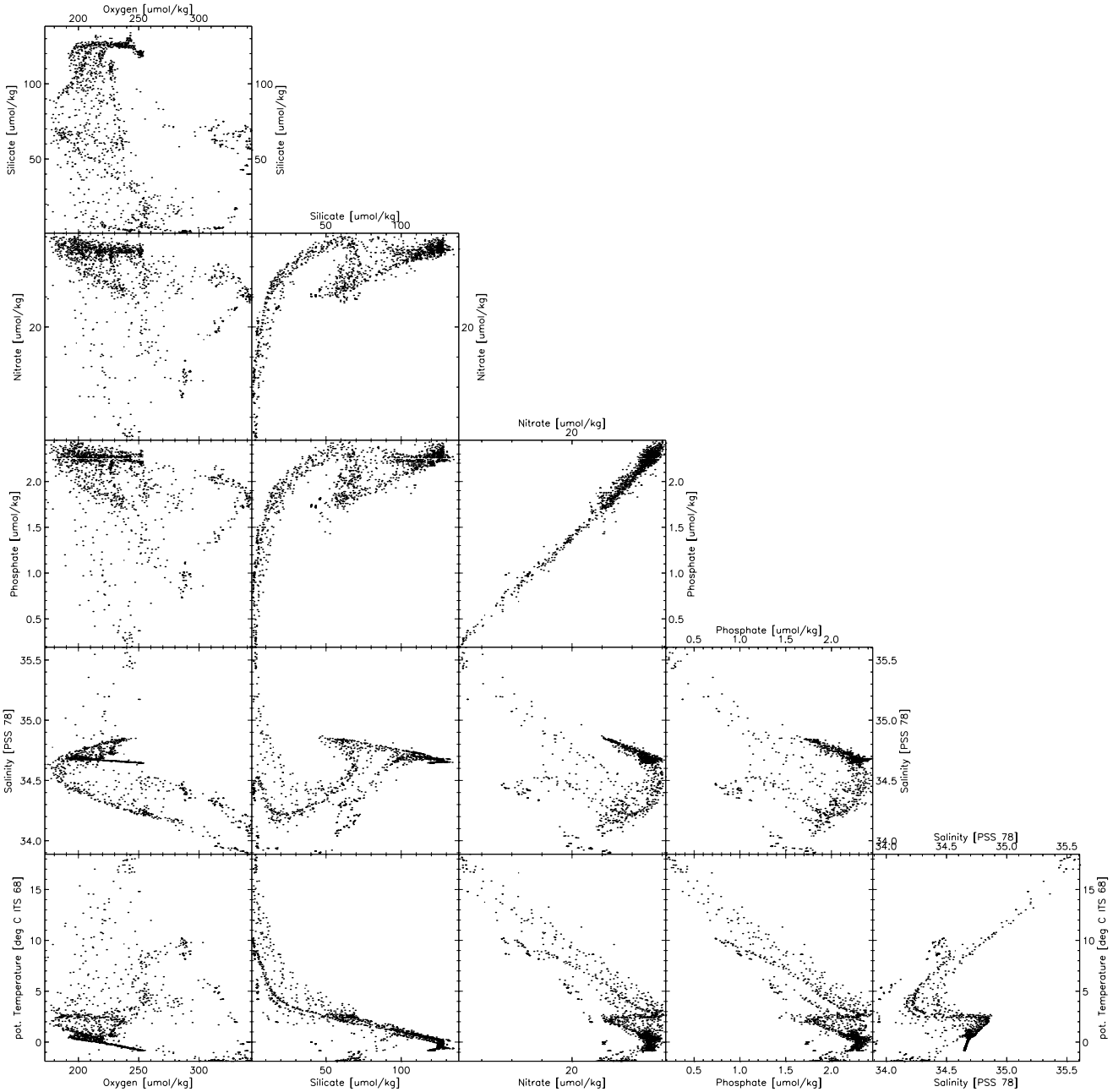

A12 preliminary (06AQANTX-4) Property-Property Matrix

WHP SAC 14/September/1995

8 May 1995

ANTX4 DQE Notes: J. C. Jennings, Jr.

The cruise track runs from Capetown, SA southwest to the Greenwich Meridian; then south to the Antarctic continental shelf. This is identified as WOCE section A12 in the ANTX4.SUM file. Then the track runs northwest to the tip of the Antarctic Peninsula, essentially repeating the WWGS89 (ANTVIII/2) and SWGS90 (ANTIX/?) sections across the central Weddell gyre. This latter part of the cruise is identified as SR04.

Overall Impressions:

There are large meridional property gradients as the southbound cruise track crosses the various Subantarctic and Polar frontal features. This is particularly evident at about 45 S where the Polar Front is encountered, and in the northwestern Weddell gyre where the outflow of very cold and fresh WSBW is concentrated.

The comments below are based on an internal comparison of the ANTX4 nutrient and dissolved oxygen data made by plotting these parameters against theta and pressure in multi-station groups. Our general criterion was to flag as questionable the bottle data that plotted outside a multi-station "envelope" by more than 1 % of the average deep water concentrations. Thus, phosphate which appeared high or low by > 0.03 uM/Kg, nitrate which was off by > 0.35 uM/Kg, etc. Almost none of the silicate data was considered questionable. This is partly because of the wide range of concentrations encountered in the Weddell Sea on this and other historical cruises. We have observed a range of silicate concentrations in the WSBW of > 40 uM/Kg in this and other Weddell Sea data, so it is difficult to argue that a high or low value near the bottom at a given station is questionable.

We also made comparisons of the ANTX4 nutrient and dissolved oxygen data with data from three other cruises. Groups of 5 - 10 stations within latitude ranges of 2 - 5 degrees were compared using plots of properties versus theta and pressure with emphasis on the deep water column where biological activity should be minimal. A summary of these comparisons is given in a separate document (WSEAHIST.WP for WordPerfect format or WSEAHIST.TXT for the same material in ASCII text).

Individual station comments: A12

Station 541:

Btls 1 - 7: Low phosphate. Flags assigned: 3

Station 542:

Btls 3 @ 4195 - 5 @ 3403 db : Low dissolved oxygen: Flags assigned: 3

Station 544:

Btl 9 @ 2198 db: All nutrients low. Flags assigned: 3

Station 545:

Btl 20 @ 241 db: Low oxygen: Flag assigned: 3

Station 553:

Btls 5, 6, & 7: All nutrients high on theta and pressure plots. Oxygen looks ok. Flags assigned: 3

Station 572:

Btl 7 @ 2200 db: High phosphate. Flag assigned: 3

Station 573:

Btls 1 - 7: Low phosphate and nitrate. No proportional increase in oxygen. Flags assigned: 3

Station 577:

Btls 4 @ 3202 db - 6 @ 2501 db: Silicate looks high on theta plot. Flags assigned: 3

Station 580:

Btl 9 @ 2204 db: High nitrate. Flag assigned: 3

Station 581:

Btl 9 @ 2198 db: High phosphate. Flag assigned: 3

Station 583:

Btls 1 @ 5442 - 7 @ 4203 db: Phosphate looks high on theta plot. Nitrate seems ok. Flags assigned: 3

Station 584:

Btl 4 @ 4799 db - 11 @ 2800 db: Nitrate looks too high. Phosphate drops at this station. Flags assigned (to Nitrate): 3

Station 585:

Btl 7 @ 3500 db: Low oxygen on theta plot. Flag assigned: 3

Station 586:

Btls 11 @ 5390 db - 21 @ 1800 db: Nitrate low on pressure an theta plots; outside "envelope" of adjacent station data. Flags assigned: 3

Station 587:

Btls 3 @ 5279 - 6 @ 3999: Nitrate looks high. Flags assigned: 3

Station 590:

Btl 12 @ 1200 db: High nitrate. Flag assigned: 3

Station 592:

Btls 3 @ 4539 db - 5 @ 3800 db: Low nitrate. Flags assigned: 3

Btls 7 @ 3000 db and 8 @ 2598 db: Low nitrate. Flags assigned: 3

Station 594:

Btls 3 @ 3775 db - 10 @ 1500 db: Nitrate looks too high: Flags assigned: 3

Station 595:

Btls 2 @ 3340 db - 8 @ 2100 db: Phosphate looks high. Oxygen all silicate look ok. Flags assigned to phosphate: 3

Btls 6 @ 2801 - 8 @ 2100 db: Nitrate looks too low. Flags assigned: 3

Station 596:

Btls 10 @ 2000 db - 13 @ 1000 db: Nitrate looks low on both pressure and theta plots: Flags assigned: 3

Btls 15 @ 700 db - 22 @ 140 db: Nitrate looks low. Flags assigned: 3

Btl 11 @ 1800: Phosphate high: Flag assigned: 3

Station 598:

Btl 8 @ 2500 db: High nitrate: flag assigned: 3

Btl 17 @ 399 db: Low nitrate: Flag assigned: 3

Station 599:
Btls 6 @ 3399 db and 7 @ 2999 db: Nitrate looks high by about 0.4 micromoles. Flags assigned: 3
Station 604:
Btl 1 @ 2592 db: Low phosphate on theta plot. Flag assigned: 3
Btl 3 @ 2401 db: High nitrate: Flag assigned: 3
Station 605:
Btl 23 @ 40 db: High phosphate. Flag assigned: 3
****
Individual station comments: SR04

Station 610:
Btl 4 @ 249 db: High phosphate. Flag assigned: 3
Station 612:
All btls: Low nitrate. Flags assigned: 3
Station 619:
Btl 10 @ 2179 db: Low nitrate. Flag assigned: 3
Station 623:
Btls 1 @ 4845 db to 3 @ 4799 db: High nitrate. Flags assigned: 3
Station 630:
Btl 15 @ 799 db: High nitrate. Flag assigned: 3
Station 635:
Btl 2 @ 628 db: High silicate by about 3 uM/Kg. Flag assigned: 3
Btl 15 @ 118 db: Low oxygen, no nutrient data. Flag assigned: 3

INPUT FILE: antx4.jcj
THE DATE TODAY IS: 11-JUL-95

STN NBR	CAST NO	SAMP NO	CTD PRS	OXYGEN	NITRAT	NITRIT	SILCAT	PHSPHT	QUALT 1	QUALT 2
541	1	7	2000.0					1.66	~~~~2	~~~~3
541	1	6	2500.2					1.56	~~~~2	~~~~3
541	1	5	2998.7					1.59	~~~~2	~~~~3
541	1	4	3499.7					1.67	~~~~2	~~~~3
541	1	3	4000.3					1.88	~~~~2	~~~~3
541	1	2	4344.0					1.96	~~~~2	~~~~3
542	1	5	3402.6	226.8					2~~~~	3~~~~
542	1	4	3800.9	221.5					2~~~~	3~~~~
542	1	3	4194.7	218.3					2~~~~	3~~~~
544	1	9	2197.5		26.38	0.05	51.10	1.74	~2222	~3333
545	1	20	241.1	208.1					2~~~~	3~~~~
553	1	7	3000.2		27.96		75.73	1.93	~2~22	~3~33
553	1	6	3400.1		30.26		94.26	2.08	~2~22	~3~33
553	1	5	3800.7		31.76		106.75	2.21	~2~22	~3~33
572	1	7	2200.3					2.18	~~~~2	~~~~3
573	1	7	1195.2		27.69			1.88	~2~~2	~3~~3
573	1	6	1398.8		27.72			1.88	~2~~2	~3~~3
573	1	5	1600.6		27.84			1.92	~2~~2	~3~~3
573	1	4	1802.4		28.34			1.93	~2~~2	~3~~3
573	1	3	2000.3		28.96			1.94	~2~~2	~3~~3
573	1	2	2127.4		29.32			1.93	~2~~2	~3~~3
573	1	1	2236.7		29.69			1.87	~2~~2	~3~~3
577	1	6	2500.8				130.20		~~~2~	~~~3~
577	1	5	2800.8				130.15		~~~2~	~~~3~
577	1	4	3201.9				127.85		~~~2~	~~~3~
580	3	9	2200.4		33.08				~2~~~	~3~~~
581	1	9	2197.8					2.39	~~~~2	~~~~3
583	3	7	4203.1					2.37	~~~~2	~~~~3
583	3	6	4602.0					2.34	~~~~2	~~~~3
583	3	5	4899.4					2.33	~~~~2	~~~~3
583	3	4	5289.9					2.32	~~~~2	~~~~3
583	3	2	5441.2					2.34	~~~~2	~~~~3
583	3	1	5442.0					2.30	~~~~2	~~~~3
584	1	13	1800.7		33.32				~2~~~	~3~~~
584	1	12	2202.0		33.17				~2~~~	~3~~~
584	1	11	2800.5		33.46				~2~~~	~3~~~
584	1	10	3399.0		33.54				~2~~~	~3~~~
584	1	8	3397.8		33.61				~2~~~	~3~~~
584	1	7	3800.1		33.52				~2~~~	~3~~~

STN NBR	CAST NO	SAMP NO	CTD PRS	OXYGEN	NITRAT	NITRIT	SILCAT	PHSPHT	QUALT 1	QUALT 2
584	1	6	4198.8		33.65				~2~~~	~3~~~
584	1	5	4598.3		33.65				~2~~~	~3~~~
584	1	4	4799.4		33.29				~2~~~	~3~~~
585	1	7	3500.4	235.3					2~~~~	3~~~~
586	3	12	1799.7		32.08				~2~~~	~3~~~
586	3	11	2199.8		31.94				~2~~~	~3~~~
586	3	10	2599.1		31.67				~2~~~	~3~~~
586	3	9	3099.4		31.72				~2~~~	~3~~~
586	3	8	3600.0		31.75				~2~~~	~3~~~
586	3	7	3894.9		31.45				~2~~~	~3~~~
586	3	6	4199.3		31.61				~2~~~	~3~~~
586	3	5	4600.7		31.71				~2~~~	~3~~~
586	3	4	5000.1		31.66				~2~~~	~3~~~
586	3	3	5319.3		31.24				~2~~~	~3~~~
586	3	2	5390.3		31.60				~2~~~	~3~~~
587	1	6	3999.2		33.28				~2~~~	~3~~~
587	1	5	4500.0		33.84				~2~~~	~3~~~
587	1	4	4998.5		33.53				~2~~~	~3~~~
587	1	3	5278.5		33.58				~2~~~	~3~~~
590	1	12	1200.3		34.40				~2~~~	~3~~~
592	3	8	2598.4		32.40				~2~~~	~3~~~
592	3	7	3000.2		32.30				~2~~~	~3~~~
592	3	5	3799.9		31.65				~2~~~	~3~~~
592	3	4	4200.6		31.60				~2~~~	~3~~~
592	3	3	4539.2		32.01				~2~~~	~3~~~
594	1	10	1499.8		34.55				~2~~~	~3~~~
594	1	9	1799.3		35.24				~2~~~	~3~~~
594	1	8	1999.2		34.84				~2~~~	~3~~~
594	1	7	2399.7		34.70				~2~~~	~3~~~
594	1	6	2799.6		33.99				~2~~~	~3~~~
594	1	5	3199.6		33.77				~2~~~	~3~~~
594	1	4	3500.1		34.18				~2~~~	~3~~~
594	1	3	3774.6		34.33				~2~~~	~3~~~
595	3	8	2100.5		32.57			2.35	~2~~2	~3~~3
595	3	7	2401.1		32.47			2.37	~2~~2	~3~~3
595	3	6	2800.9		32.32			2.35	~2~~2	~3~~3
595	3	5	3000.9					2.32	~~~~2	~~~~3
595	3	4	3101.5					2.31	~~~~2	~~~~3
595	3	3	3270.3					2.34	~~~~2	~~~~3
595	3	2	3339.9					2.32	~~~~2	~~~~3
596	1	22	140.1		31.87				~2~~~	~3~~~
596	1	19	249.0		31.59				~2~~~	~3~~~

STN NBR	CAST NO	SAMP NO	CTD PRS	OXYGEN	NITRAT	NITRIT	SILCAT	PHSPHT	QUALT 1	QUALT 2
596	1	18	299.9		31.16				~2~~~	~3~~~
596	1	17	399.3		31.01				~2~~~	~3~~~
596	1	16	599.5		31.16				~2~~~	~3~~~
596	1	15	699.7		31.25				~2~~~	~3~~~
596	1	13	999.8		31.21				~2~~~	~3~~~
596	1	12	1199.7		31.80				~2~~~	~3~~~
596	1	11	1799.6		31.81			2.35	~2~~2	~3~~3
596	1	10	2001.1		31.92				~2~~~	~3~~~
598	3	17	399.4		31.38				~2~~~	~3~~~
598	3	8	2499.9		34.16				~2~~~	~3~~~
599	1	7	2999.2		33.96				~2~~~	~3~~~
599	1	6	3399.1		33.71				~2~~~	~3~~~
604	1	3	2400.6		33.54				~2~~~	~3~~~
604	1	1	2591.8					2.24	~~~~2	~~~~3
605	1	23	39.7					2.13	~~~~2	~~~~3
610	1	4	249.4					2.03	~~~~2	~~~~3
612	1	24	3.0		26.60				~2~~~	~3~~~
612	1	22	48.2		27.15				~2~~~	~3~~~
612	1	21	70.2		27.19				~2~~~	~3~~~
612	1	20	100.0		26.59				~2~~~	~3~~~
612	1	18	150.0		27.56				~2~~~	~3~~~
612	1	17	200.6		27.67				~2~~~	~3~~~
612	1	15	300.3		27.86				~2~~~	~3~~~
612	1	13	499.7		28.25				~2~~~	~3~~~
612	1	12	499.4		28.23				~2~~~	~3~~~
612	1	11	599.3		28.57				~2~~~	~3~~~
612	1	10	700.3		29.80				~2~~~	~3~~~
612	1	9	750.2		29.26				~2~~~	~3~~~
612	1	8	800.9		29.79				~2~~~	~3~~~
612	1	7	850.4		30.06				~2~~~	~3~~~
612	1	6	900.8		30.68				~2~~~	~3~~~
612	1	5	1000.7		30.91				~2~~~	~3~~~
612	1	4	1100.6		30.02				~2~~~	~3~~~
612	1	3	1199.5		30.58				~2~~~	~3~~~
612	1	2	1349.9		30.55				~2~~~	~3~~~
612	1	1	1430.2		30.75				~2~~~	~3~~~
619	1	10	2179.1		33.29				~2~~~	~3~~~
623	3	3	4799.0		34.15				~2~~~	~3~~~
623	3	2	4845.2		34.15				~2~~~	~3~~~
630	3	15	798.5		34.50				~2~~~	~3~~~
635	1	15	118.1	246.4					2~~~~	3~~~~
635	3	2	627.5				129.98		~~~2~	~~~3~

FIGURES

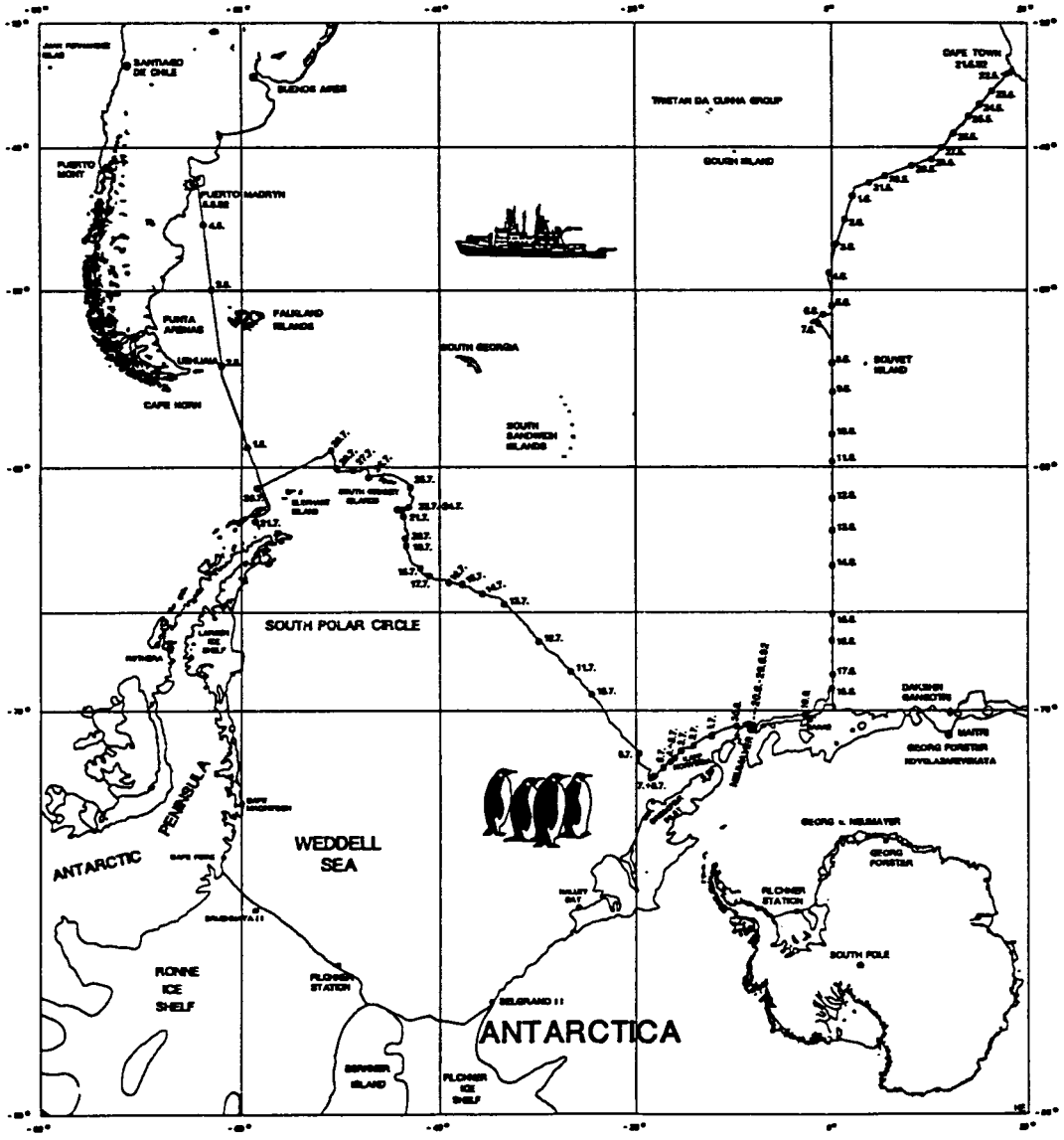

Fig. 1.1-1: Cruise track of RV “Polarstern” during ANT X/4

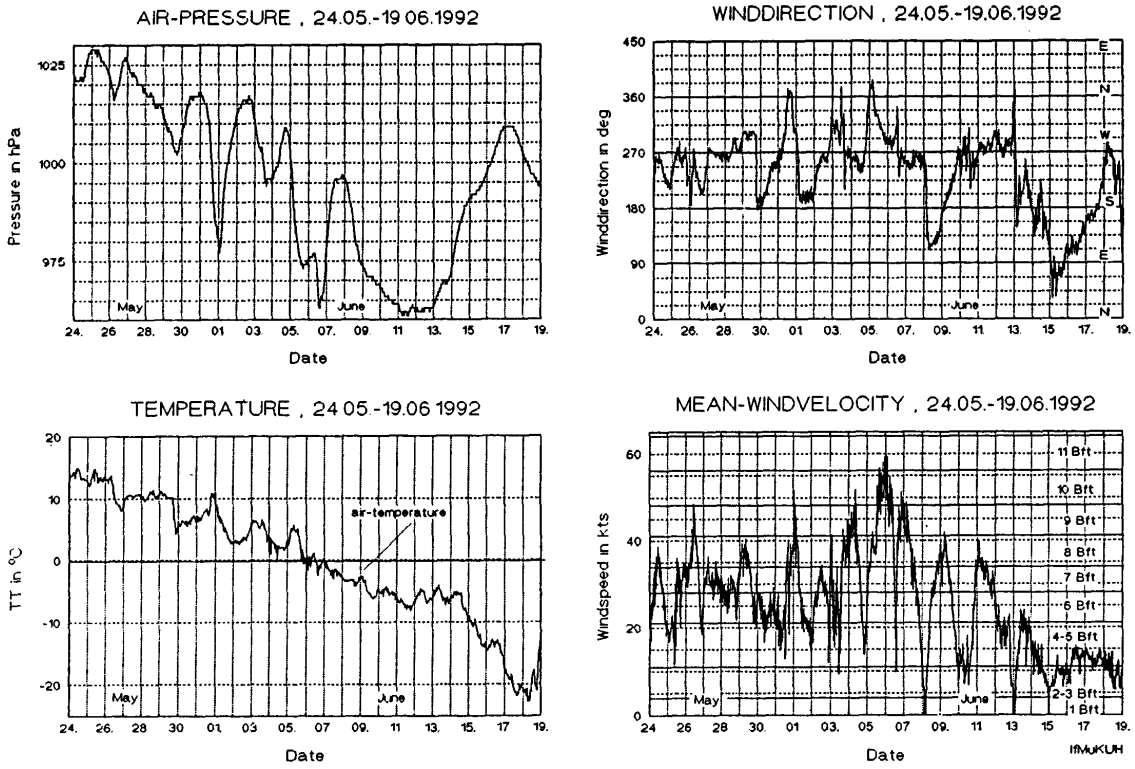

Fig. 1.3-1a: Plot of air pressure, temperature, wind direction and wind velocity for the time periods 24 May – 19 June 1992

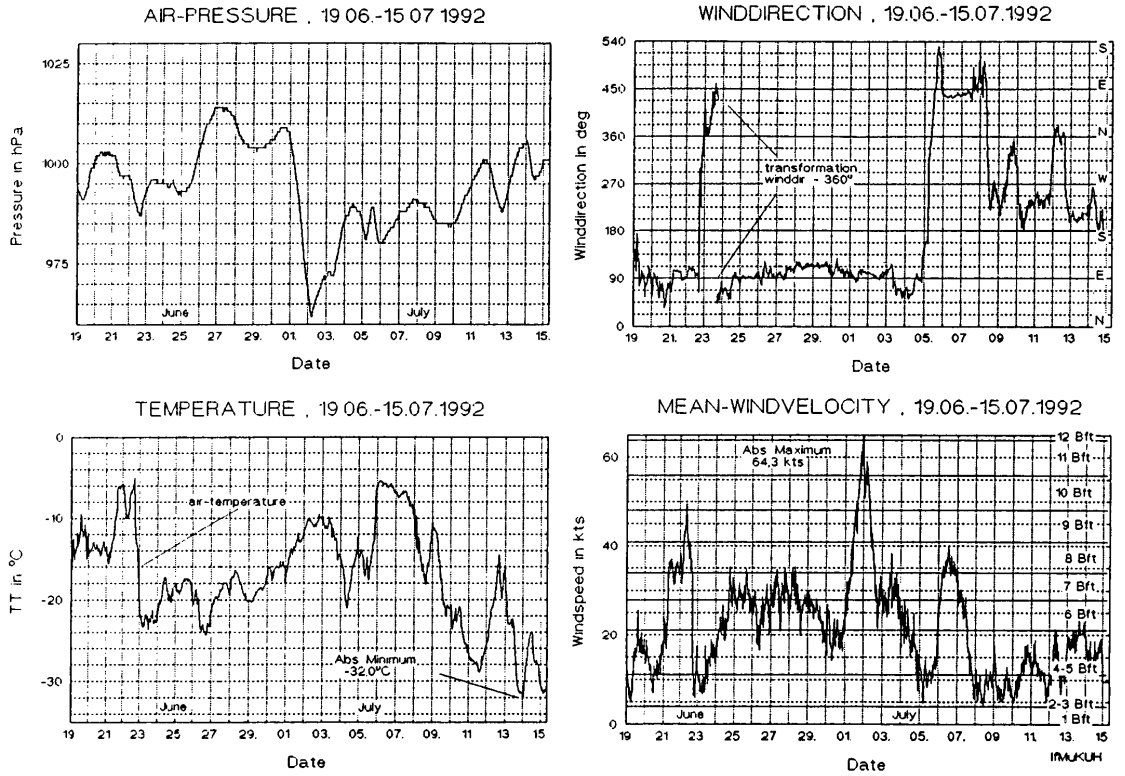

Fig. 1.3-1b: Plot of air pressure, temperature, wind direction and wind velocity for the time periods 19 June – 15 July 1992

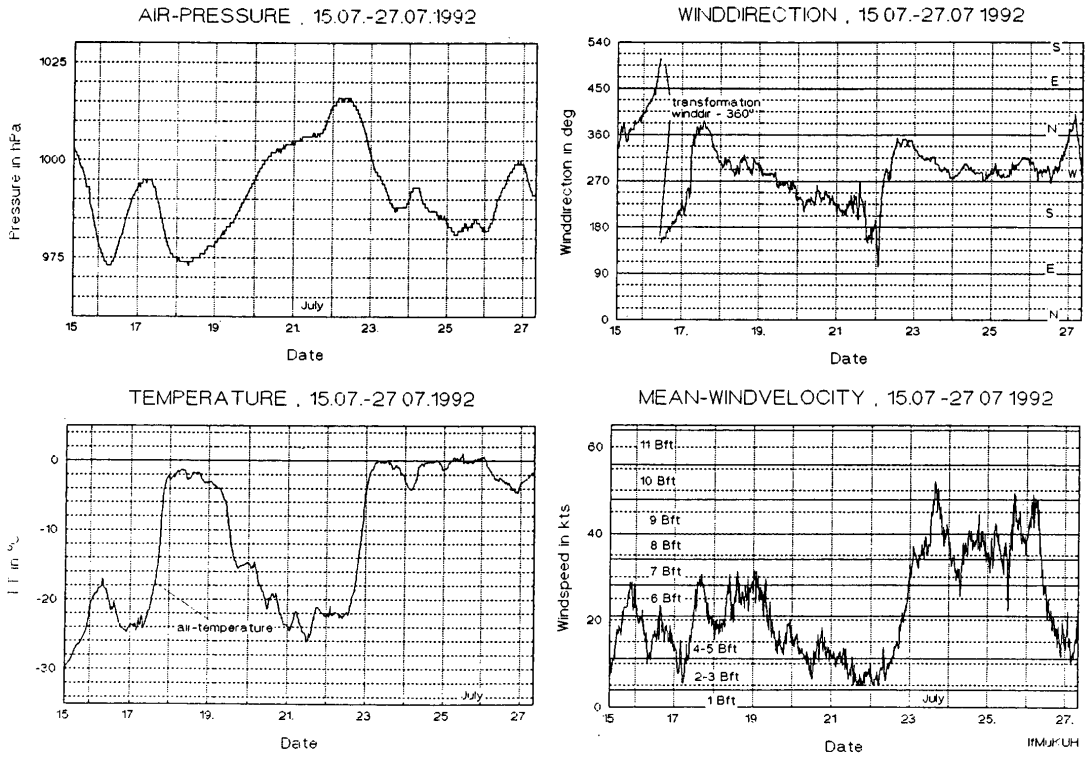

Fig. 1.3-1c: Plot of air pressure, temperature, wind direction and wind velocity for the time periods 15 July – 27 July 1992

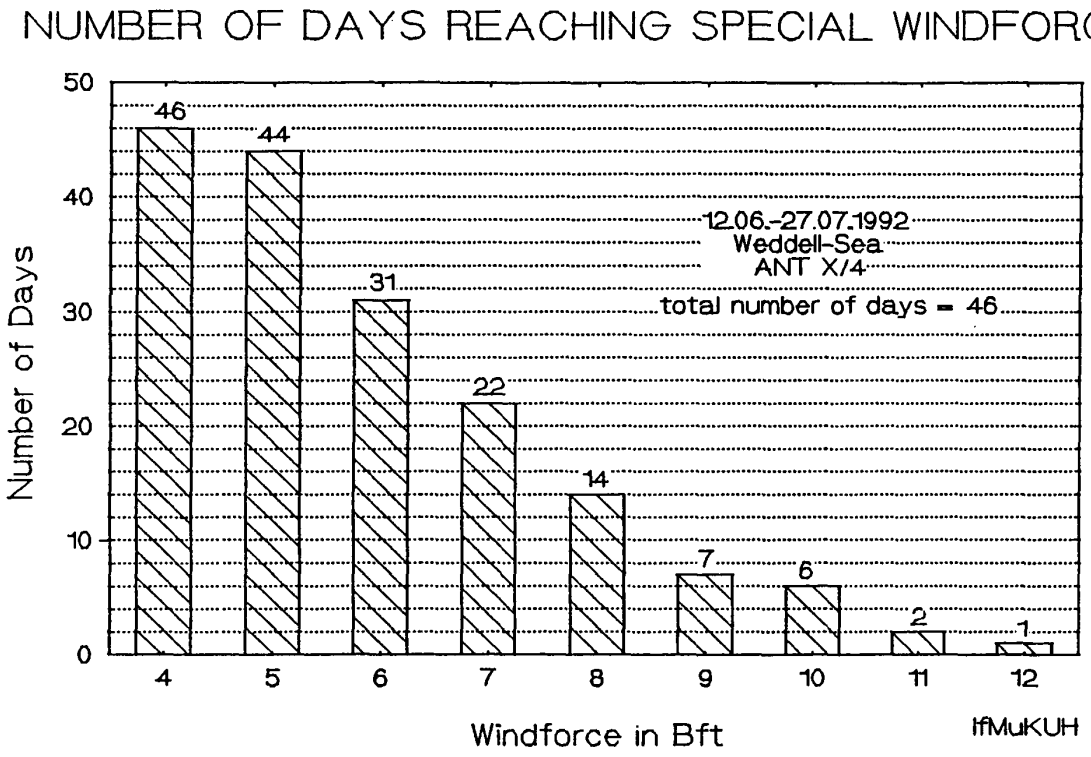

Fig. 1.3-2: Wind statistics

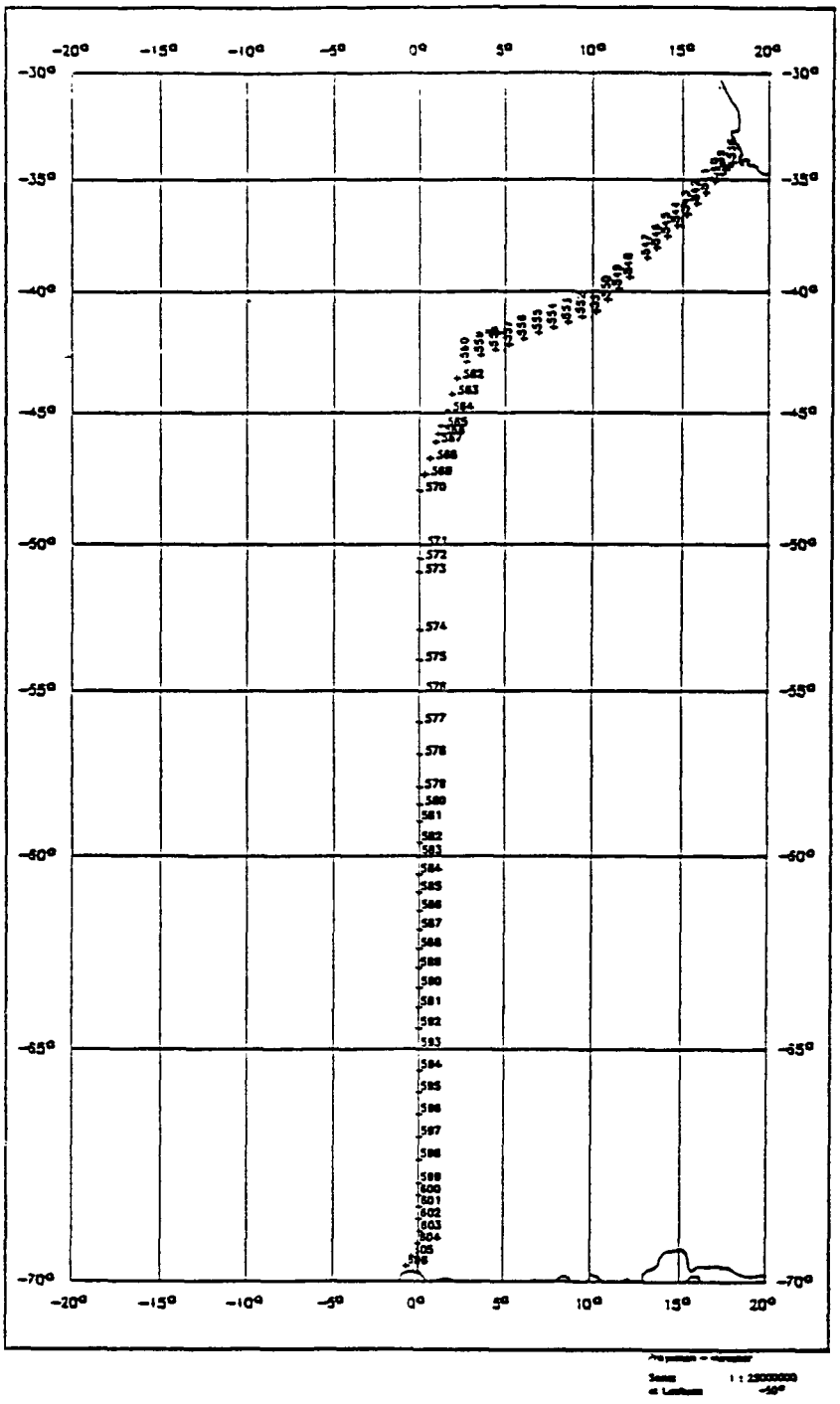

Fig. 2.1-1: ANT X/4 cruise track and station map between Cape Town and Antarctica along the Greenwich meridian

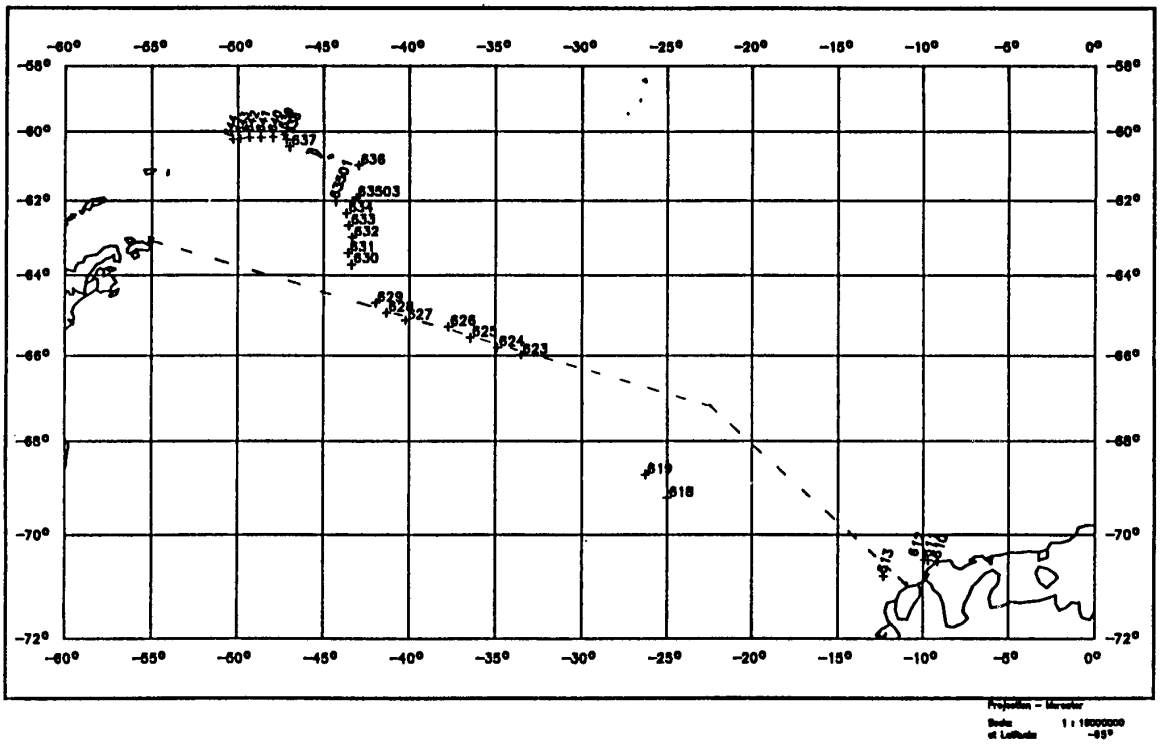

Fig. 2.1-2: Map of CTD Stations in the Weddell Sea. The broken line denotes the planned cruise track.

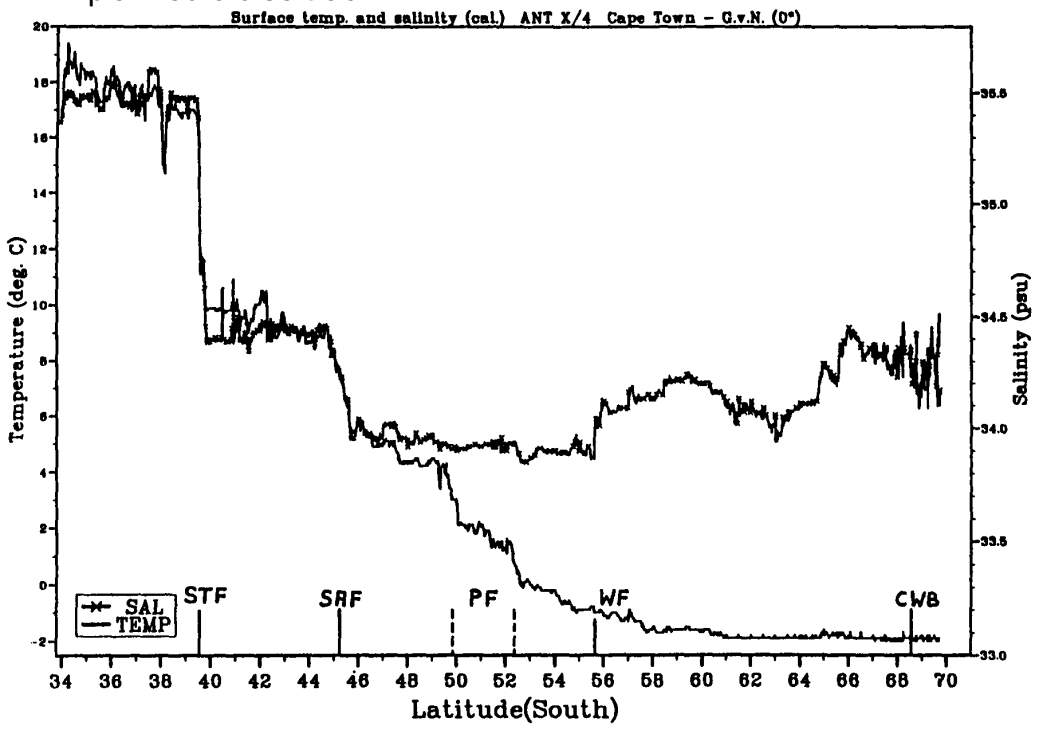

Fig. 2.1-3: Surface temperature and salinity measured with the shop's thermosalinograph at 0˚E. Marked are the position of fronts: STF= Subtropical Front, SAF= Subantarctic Front, PF= Polar Front, WF= Weddell Front, CWB= Continental Water Boundary.

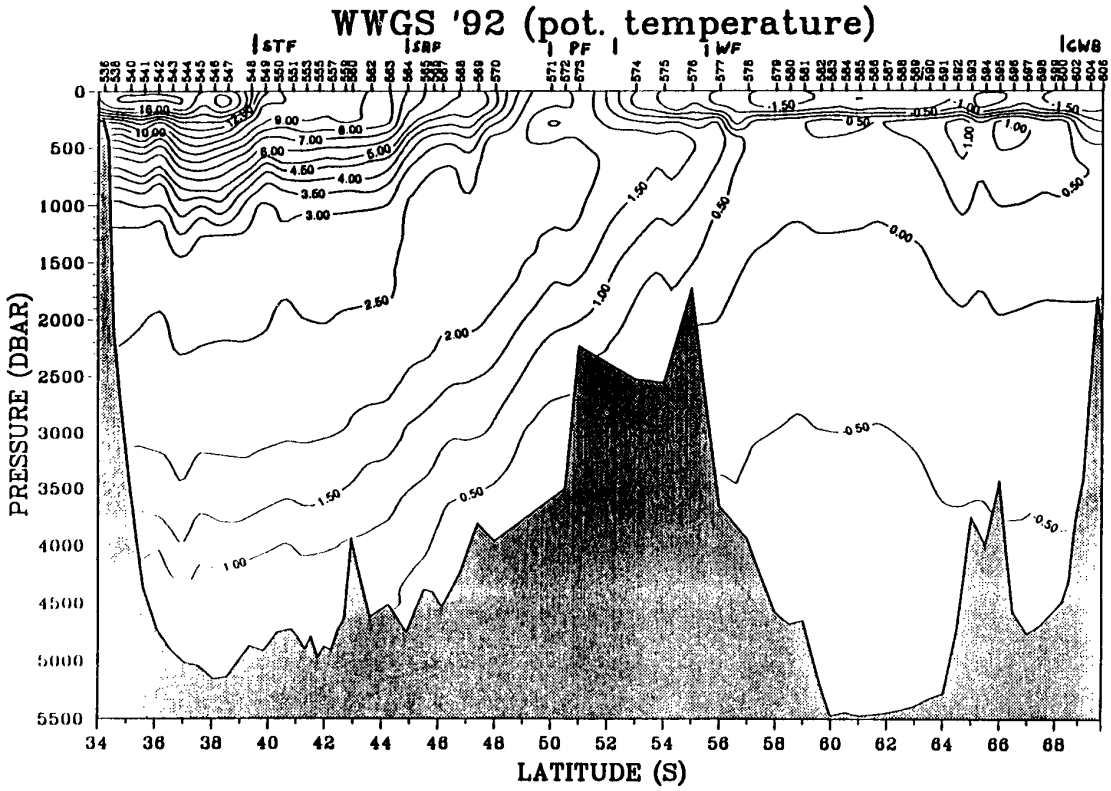

Fig. 2.1-4a: Section of potential temperature along 0˚E together with frontal positions

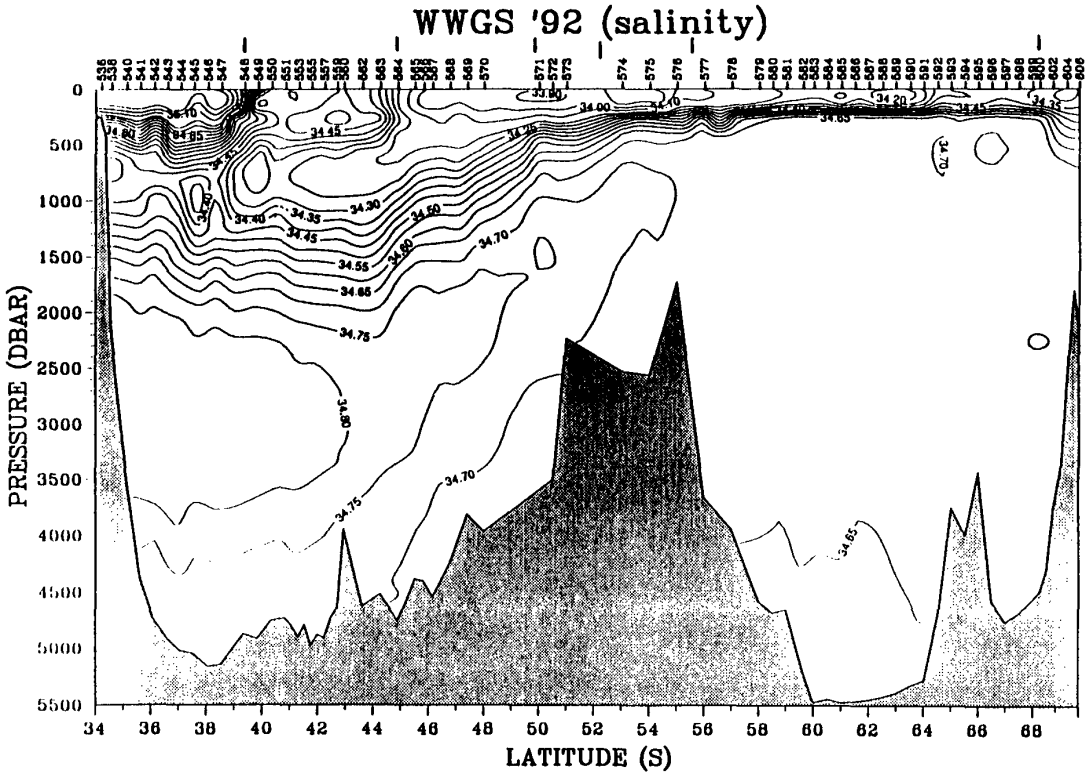

Fig. 2.1-4b: Section of salinity along 0˚E together with frontal positions

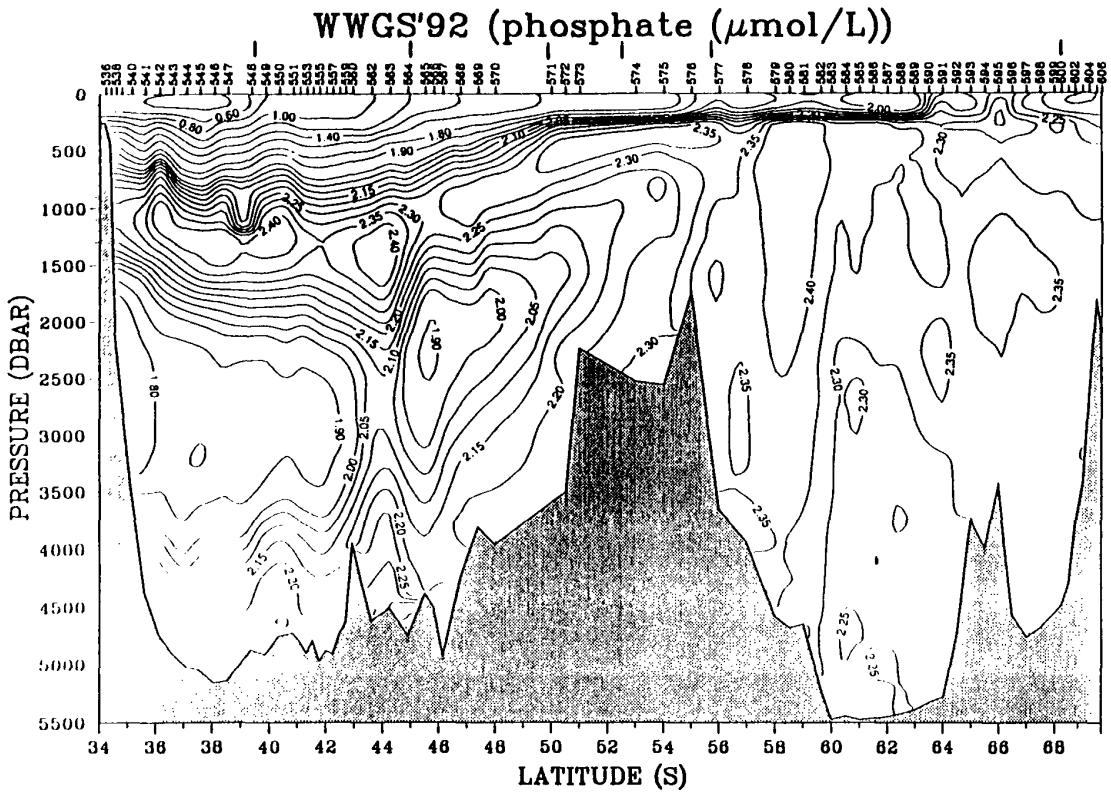

Fig. 2.1-4c: Section of phosphate along 0˚E together with frontal positions

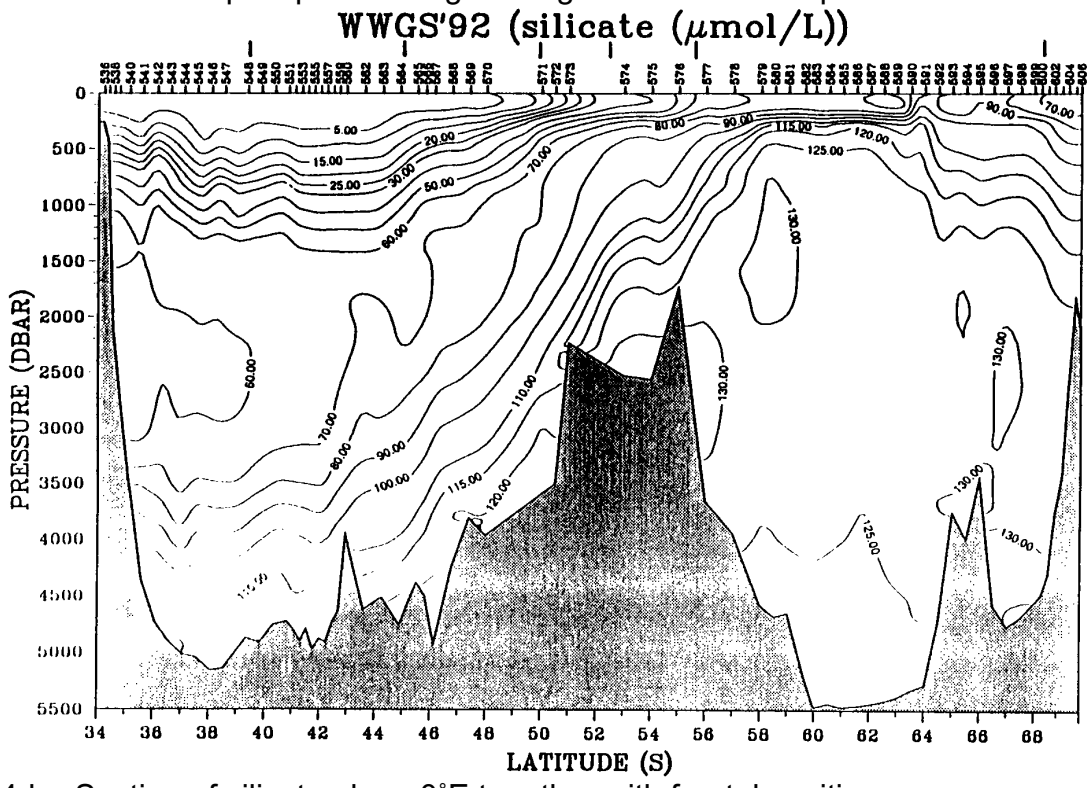

Fig. 2.1-4d: Section of silicate along 0˚E together with frontal positions

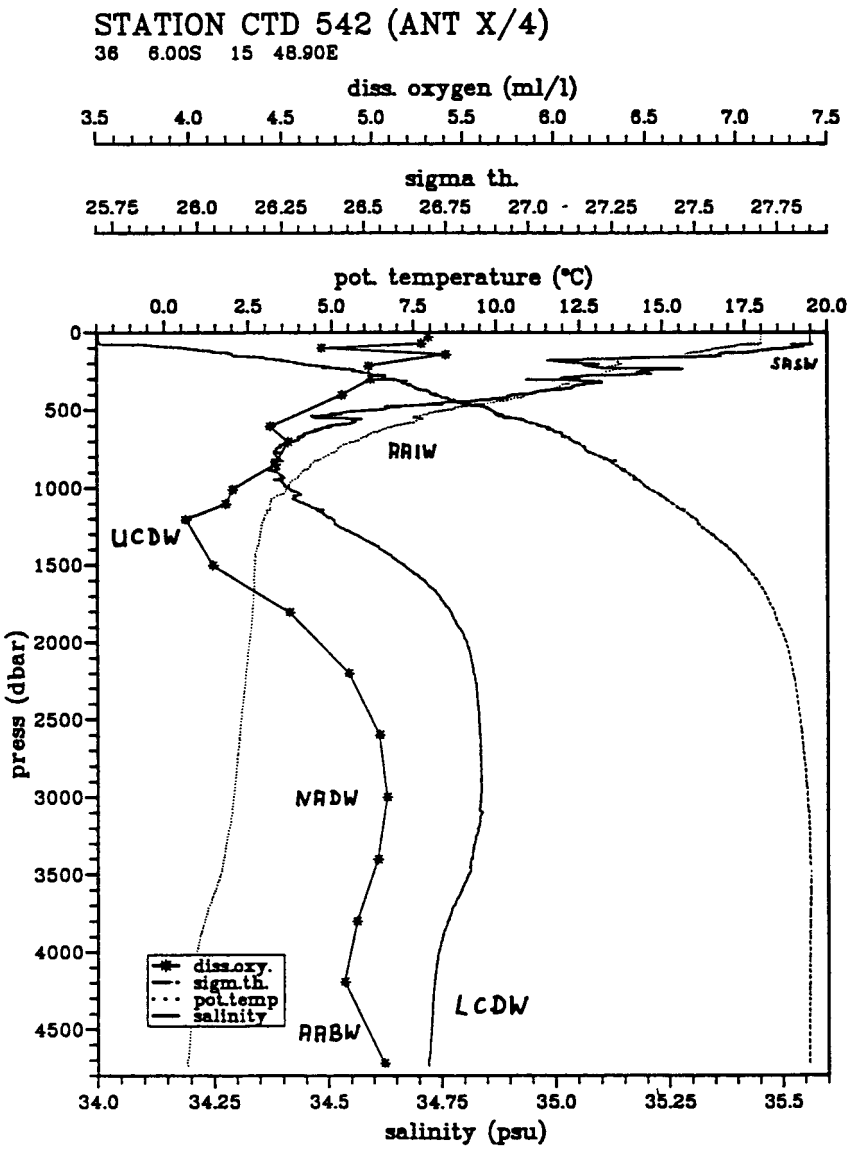

Fig. 2.1-5a: Profiles of potential temperature, salinity, dissolved oxygen, and density of station a) 542, and b) 601 which show some of the main water masses and their vertical extent in the Southern Ocean and the Weddell Gyre.

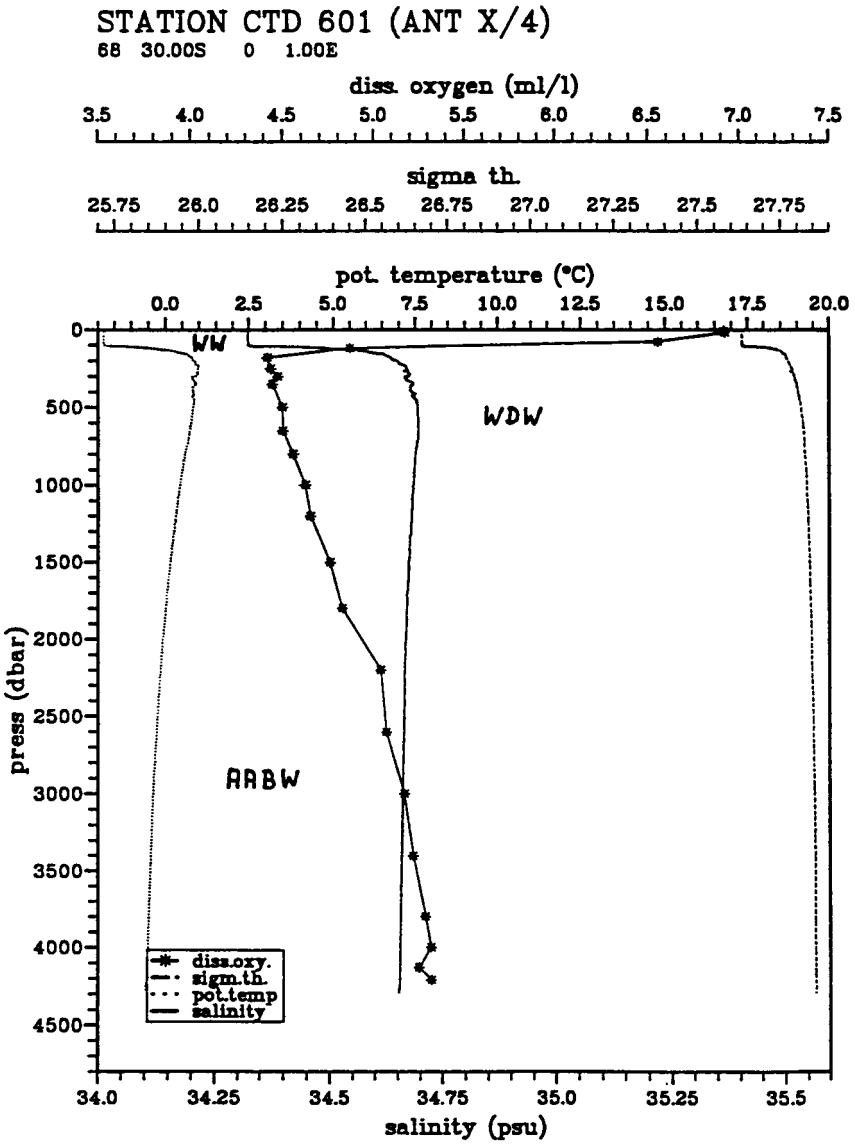

Fig. 2.1-5b: Profiles of potential temperature, salinity, dissolved oxygen, and density of station a) 542, and b) 601 which show some of the main water masses and their vertical extent in the Southern Ocean and the Weddell Gyre.

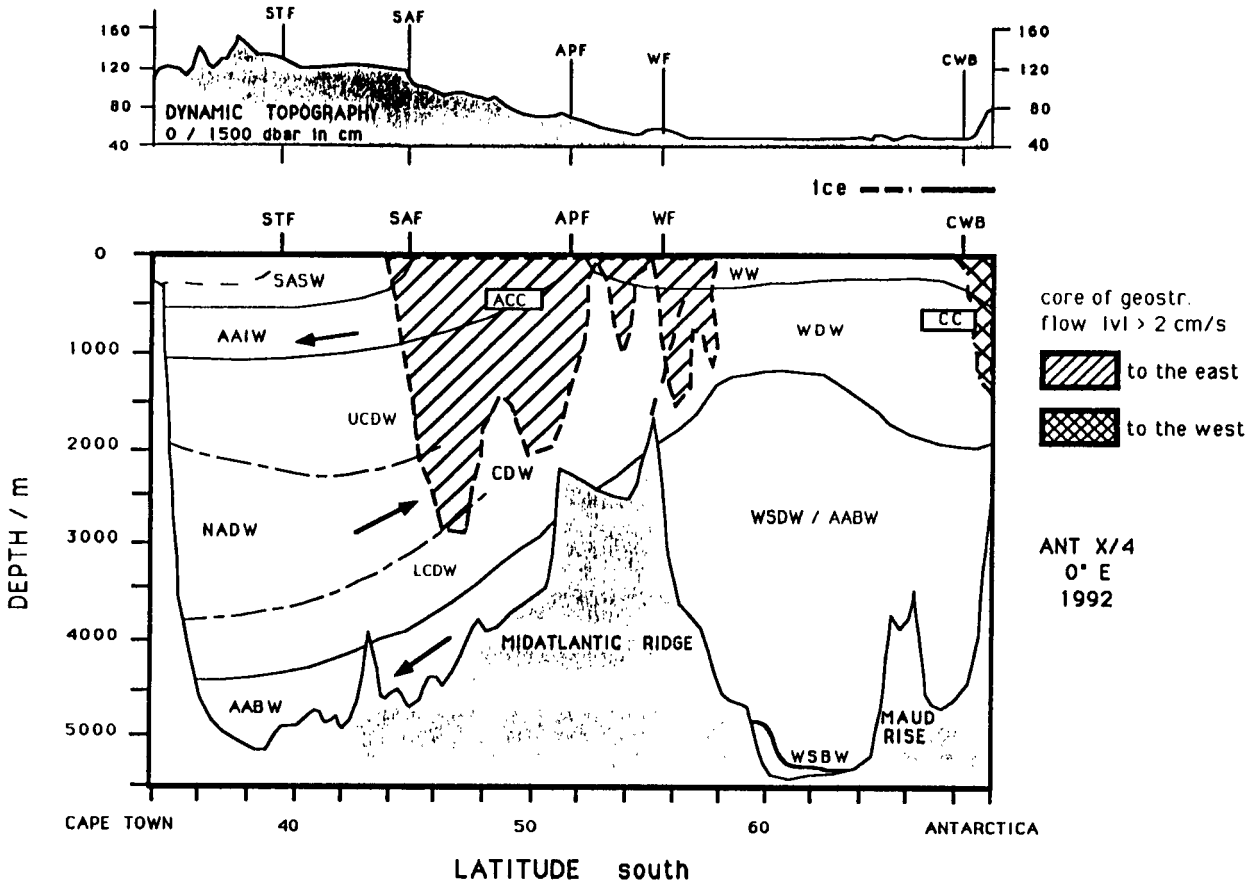

Fig. 2.1-6: Overview of the horizontal distribution water masses along 0˚E. SASWW: Subantarctic Surface Water, AAIW: Antarctic Intermediate Water, NADW: North Atlantic Deep Water, AABW: Antarctic Bottom Water, CDW: Circumpolar Deep Water (U: upper, L: lower), WW: Winter Water, WDW: Warm Deep Water, WSDW: Weddell Sea Deep Water, WSBW: Weddell Sea Bottom Water. In addition of the position of fronts, ice cover and main currents are shown, where ACC means Antarctic Circumpolar Current and CC is the Coastal Current at the antarctic shelf. In the upper panel the dynamic topography of the surface relative to 1500 dbar is shown.

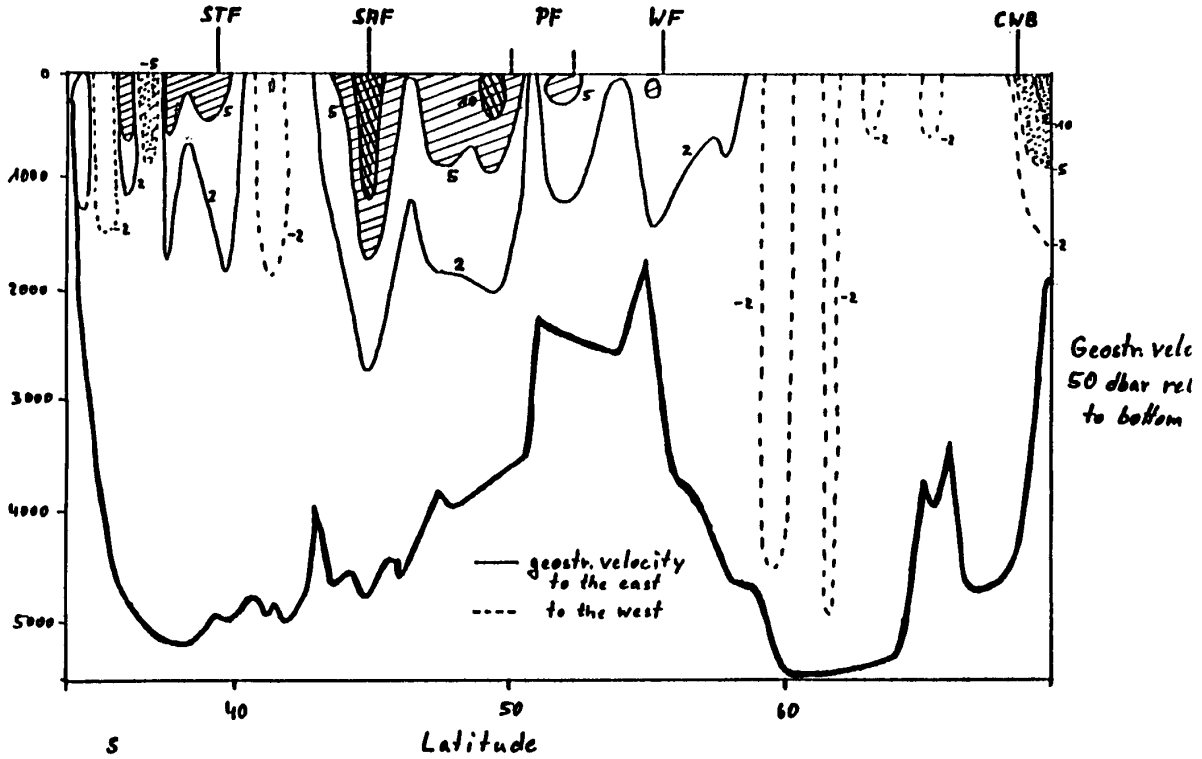

Fig. 2.1-7: Distribution of geostrophic velocities along 0˚E, calculated for the 50 dbar level relative to the bottom. Isolines of 2, 5, and 10 cm/s are shown.

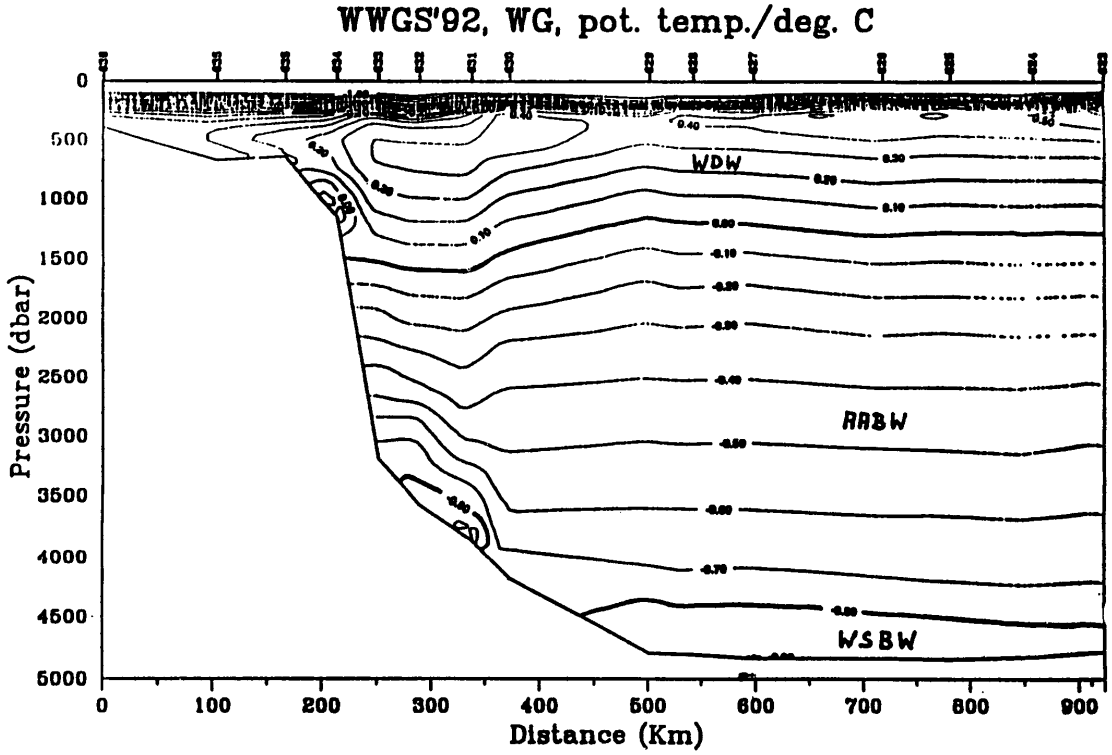

Fig. 2.1-8a: Sections of potential temperature from South Orkney (left) to the center of the Weddell Gyre (right). See also Fig. 2.1-2 for station numbers.

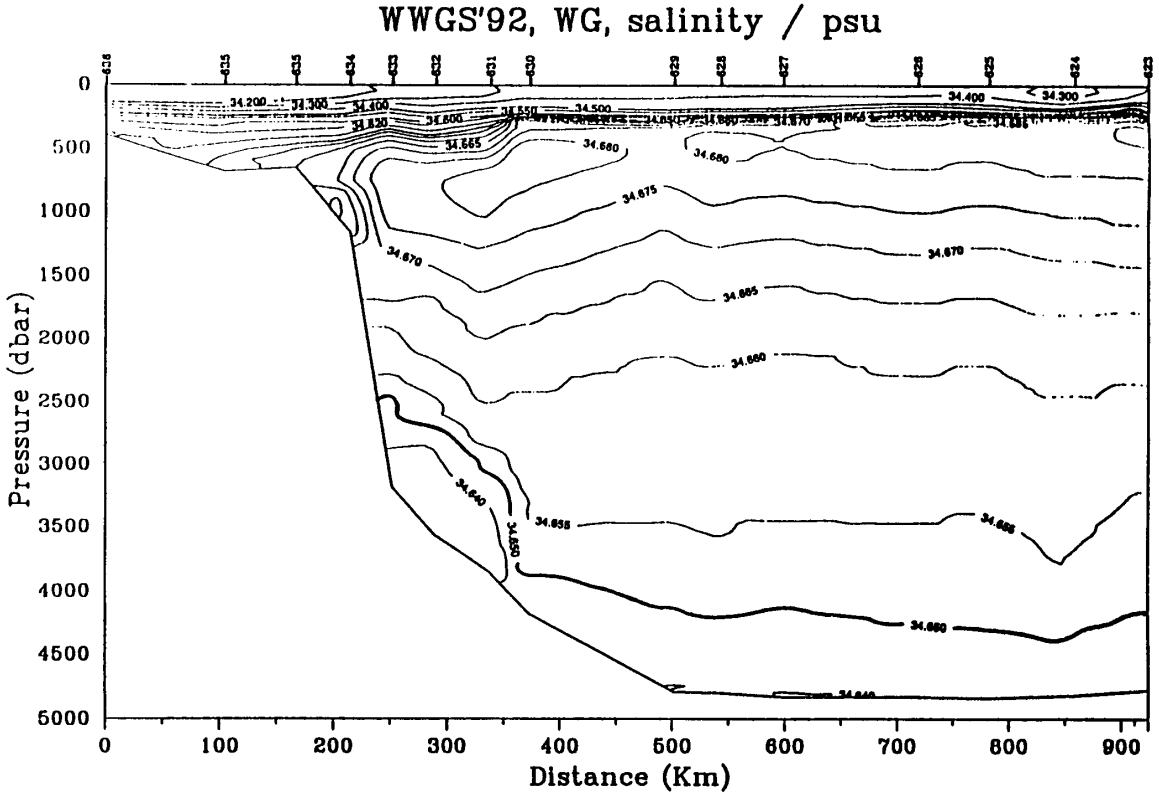

Fig. 2.1-8b: Sections of salinity from South Orkney (left) to the center of the Weddell Gyre (right). See also Fig. 2.1-2 for station numbers.

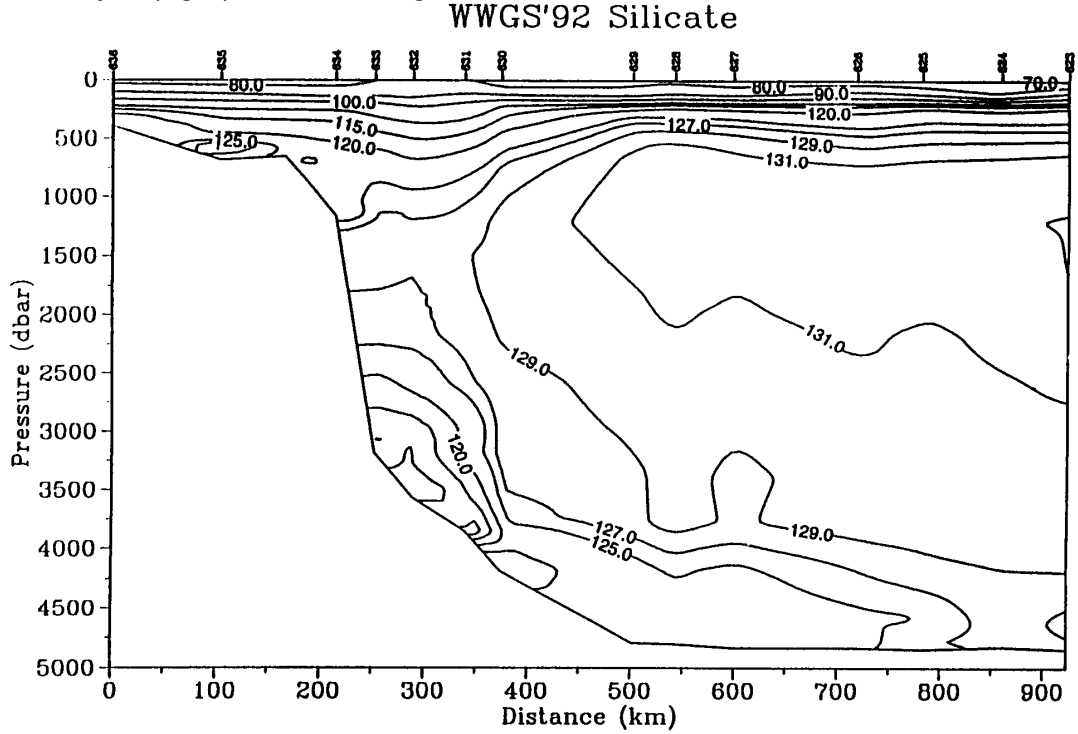

Fig. 2.1-8c: Sections of silicate from South Orkney (left) to the center of the Weddell Gyre (right). See also Fig. 2.1-2 for station numbers.

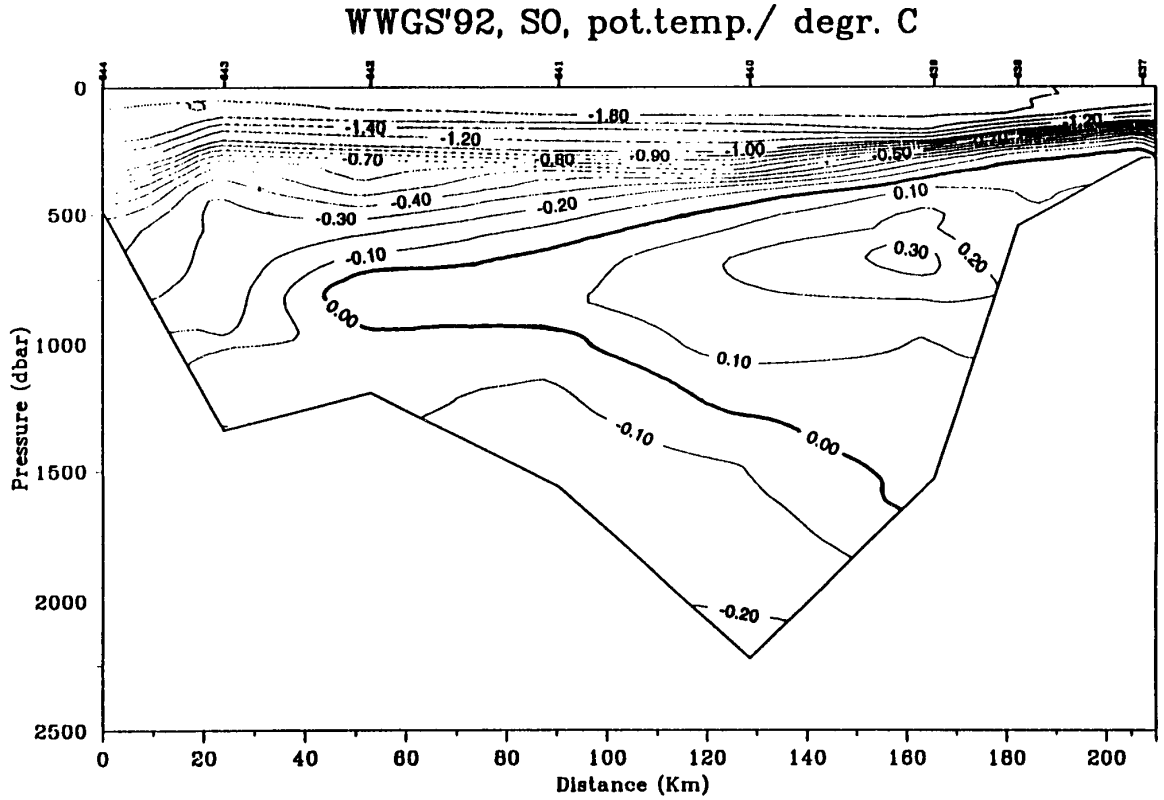

Fig. 2.1-9a: Section of potential temperature west of South Orkney. See also Fig. 2.1-2.

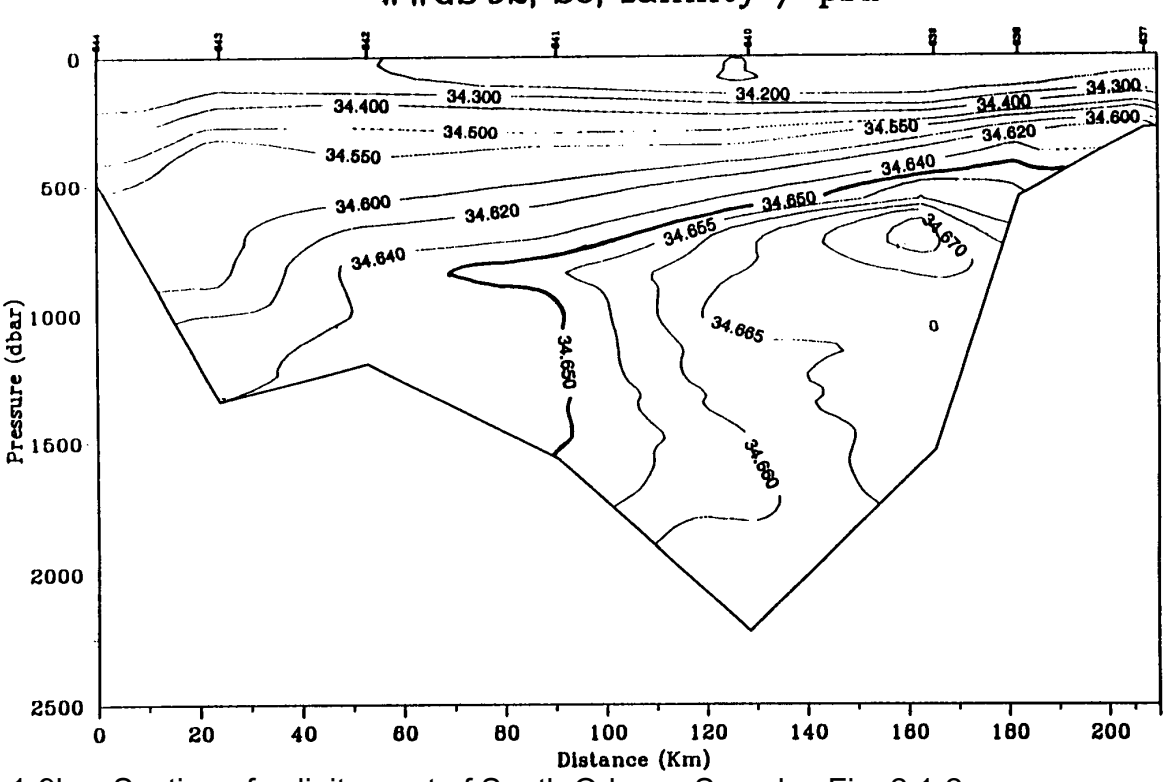

Fig. 2.1-9b: Section of salinity west of South Orkney. See also Fig. 2.1-2.

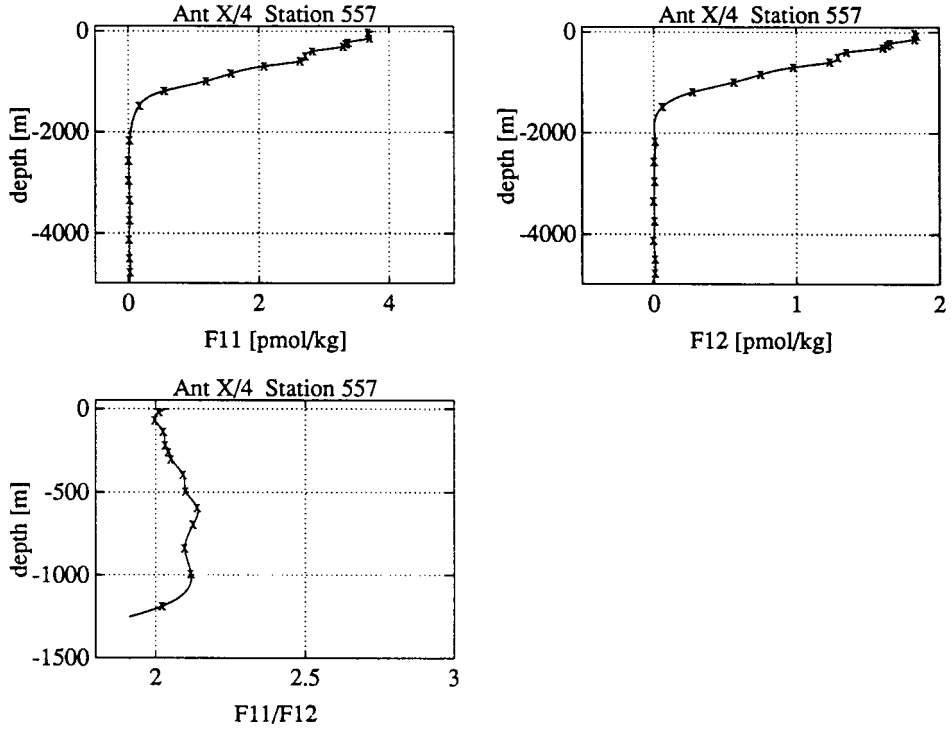

Fig. 2.1-10: Vertical profiles of Freon-11, Freon-12 and the ratio F11/F12 for Station 557.

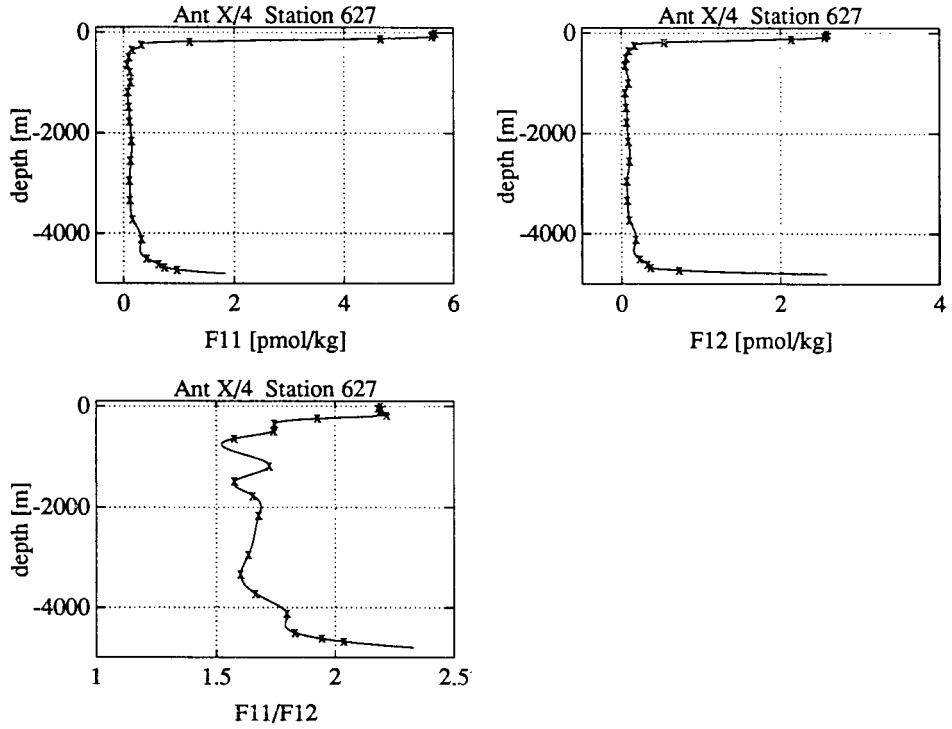

Fig. 2.1-11: Vertical profiles of Freon-11, Freon-12 and the ratio F11/F12 for Station 627.

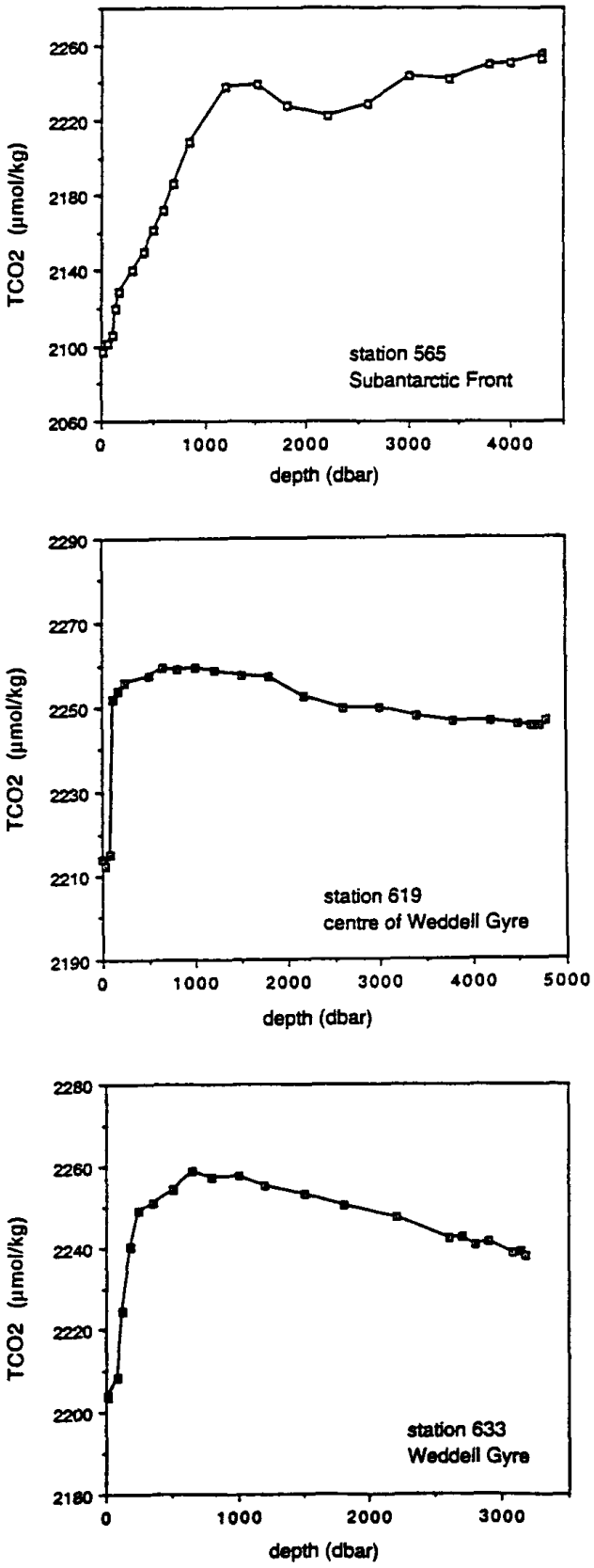

Fig. 2.1-12: Three TCO_2-depth profiles as obtained during WWGS'92

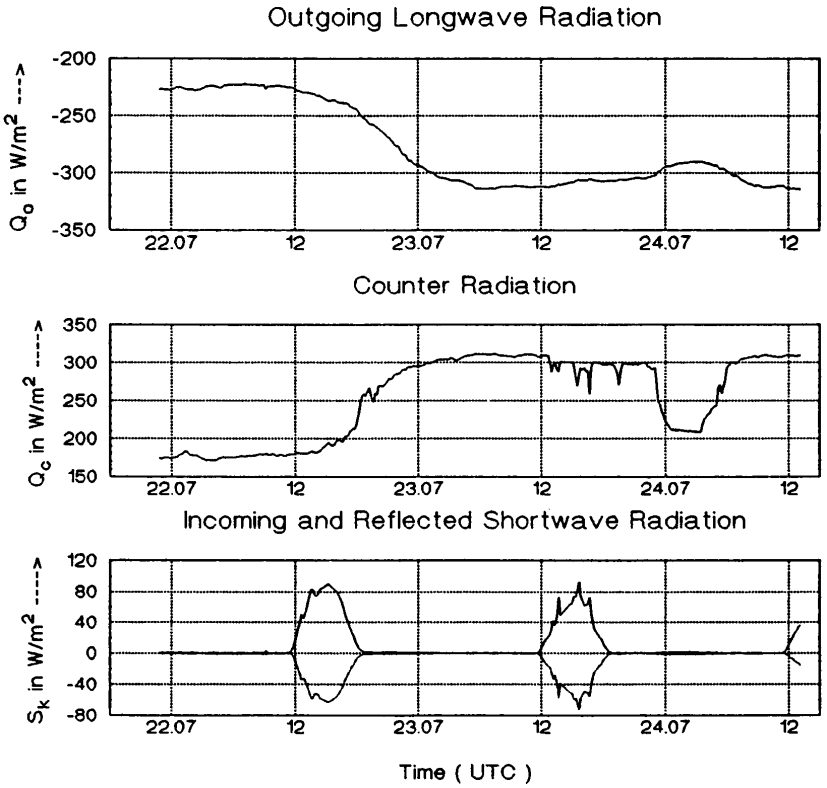

Fig. 2.2-1: Outgoing longwave radiation, counter radiation, incoming and reflected shortwave radiation during the long ice station (21 – 27 July 1992)

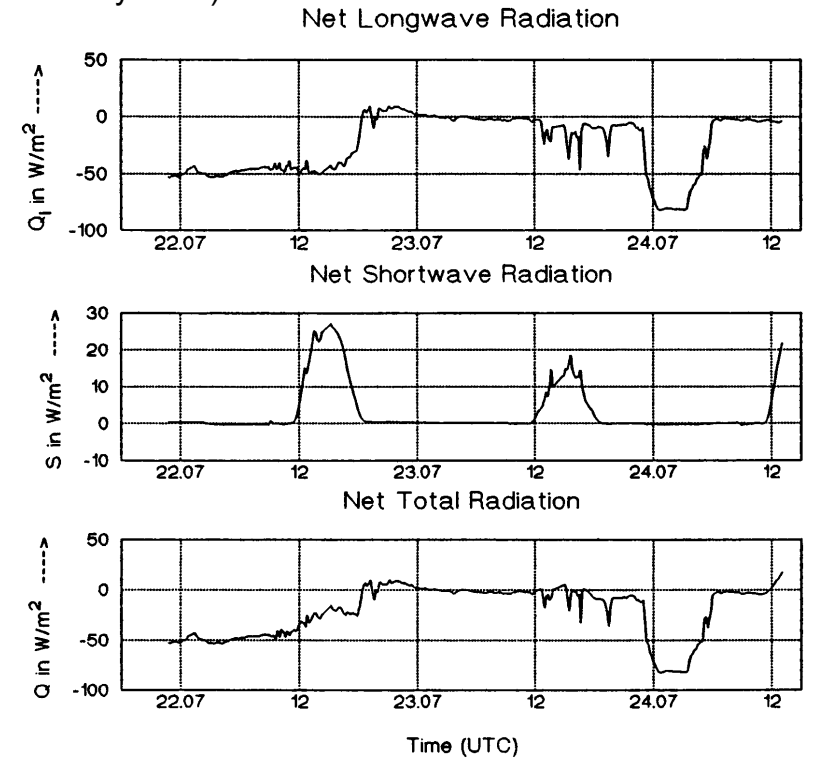

Fig. 2.2-2: Net longwave, net shortwave and net total radiation during the long ice station.

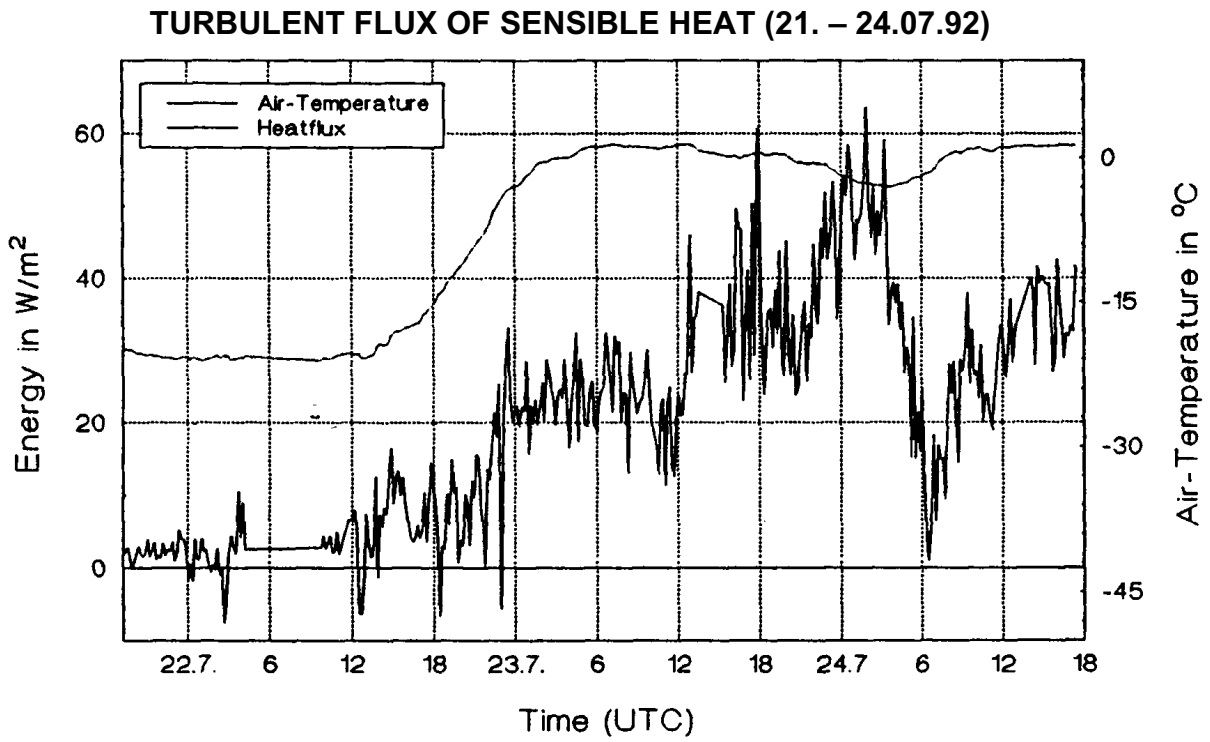

Fig. 2.2-3: Turbulent flux of sensible heat during the long ice station.

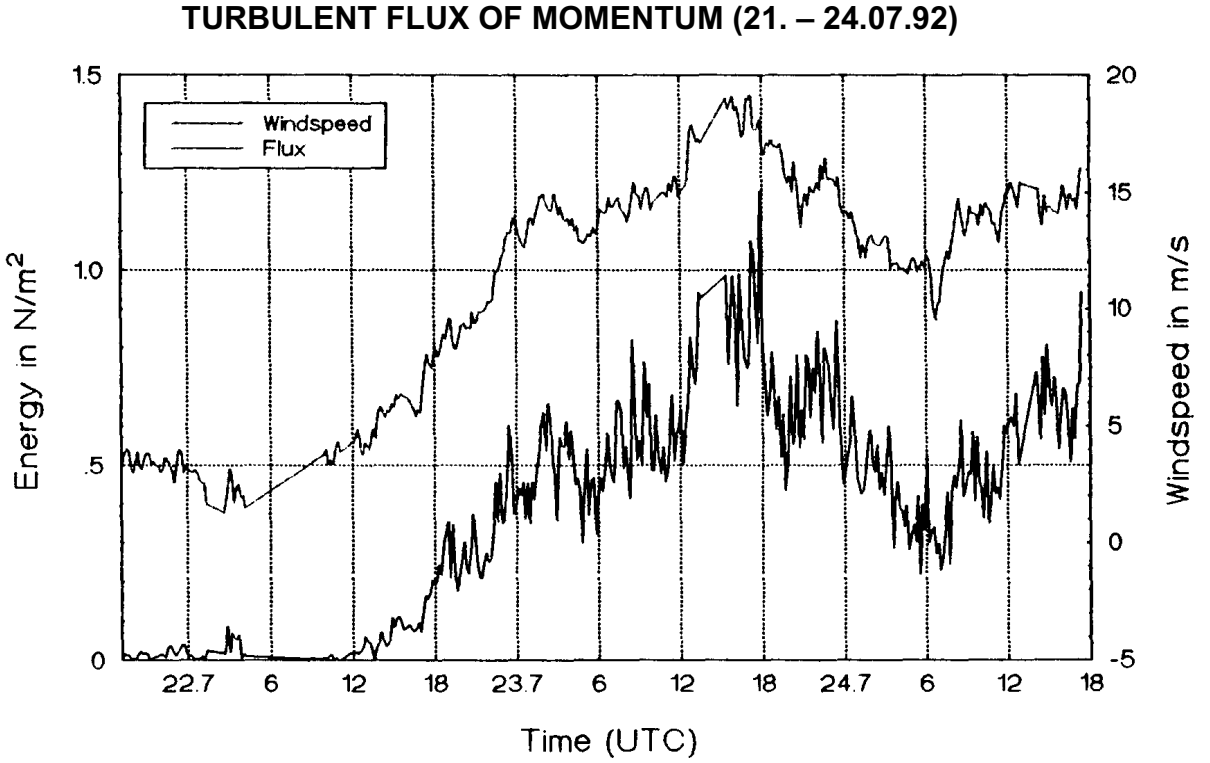

Fig. 2.2-4: Turbulent flux of momentum during the long ice station.

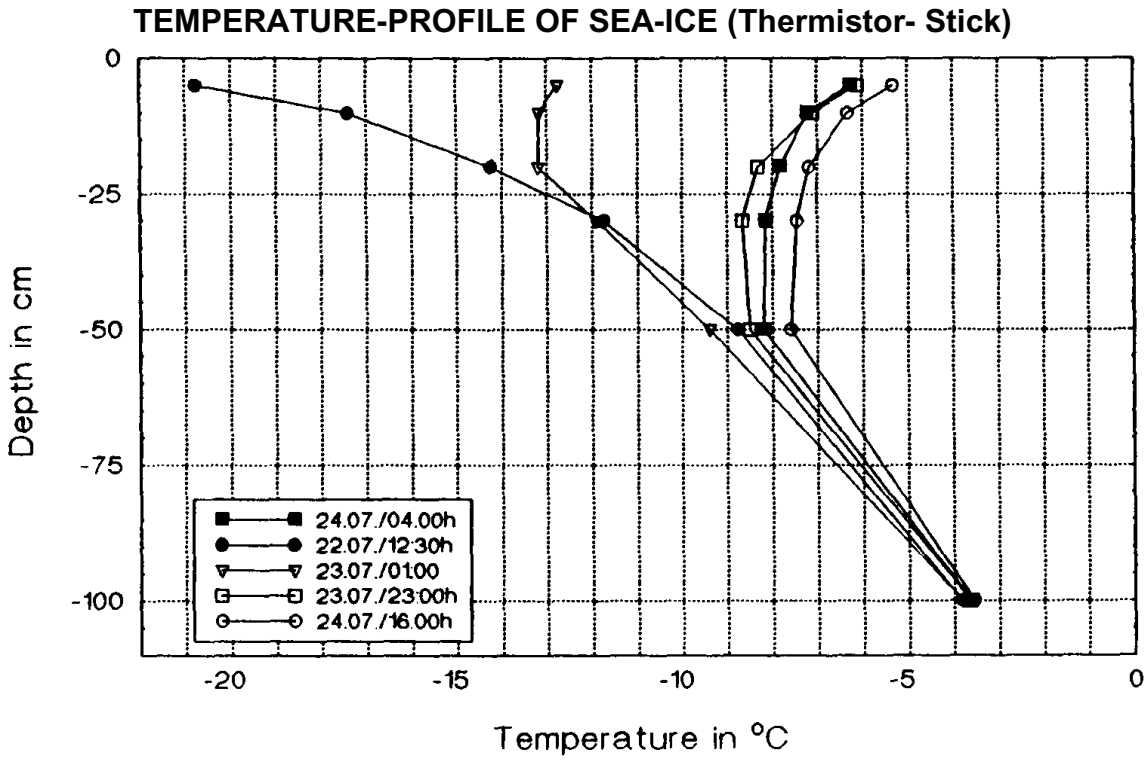

Fig. 2.2-5: Temperature profiles in the ice during the long ice station.

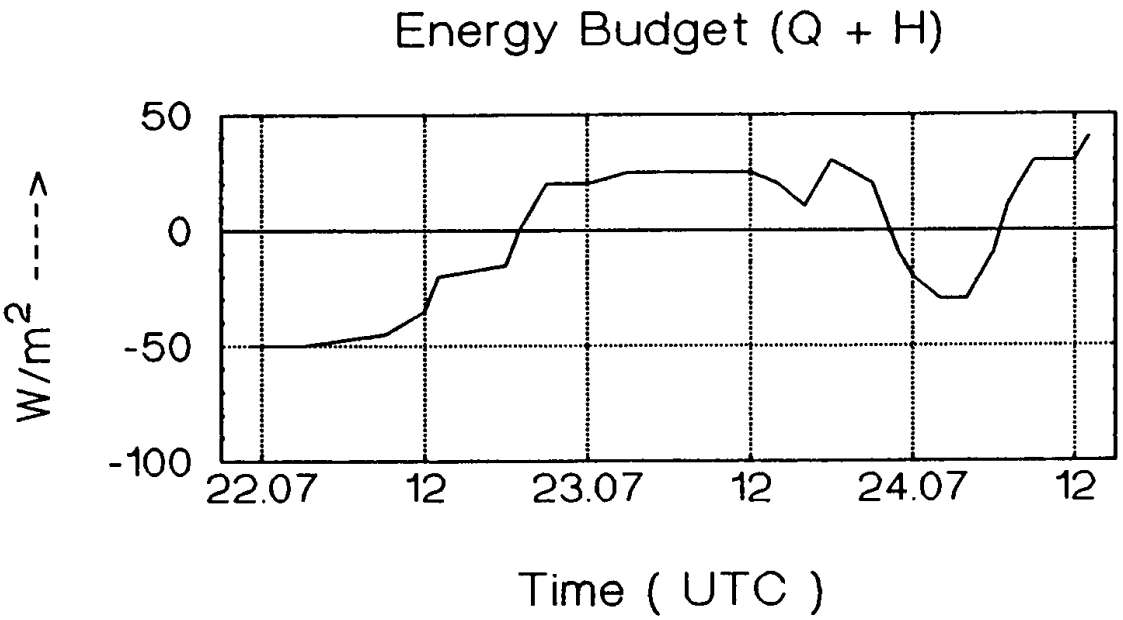

Fig. 2.2-6: Energy budget (radiation budget and turbulent flux of sensible heat) during the long ice station.

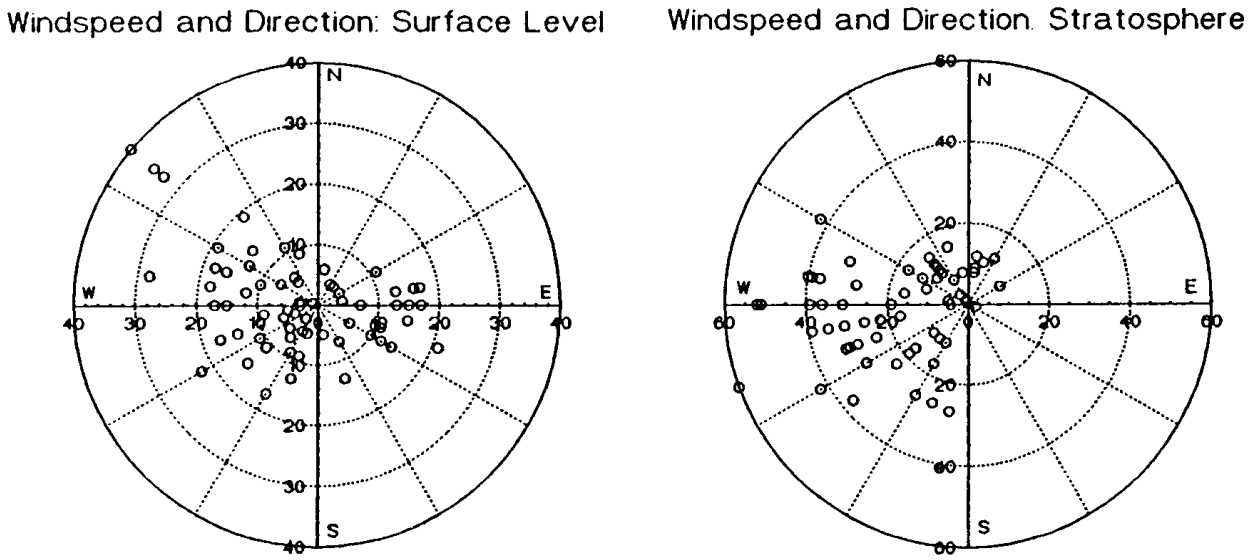

Fig. 2.2-7: Windspeed and directions at surface level and in the stratosphere from aerological oundings (12:00 UTS; 23.05. – 27.07.92)

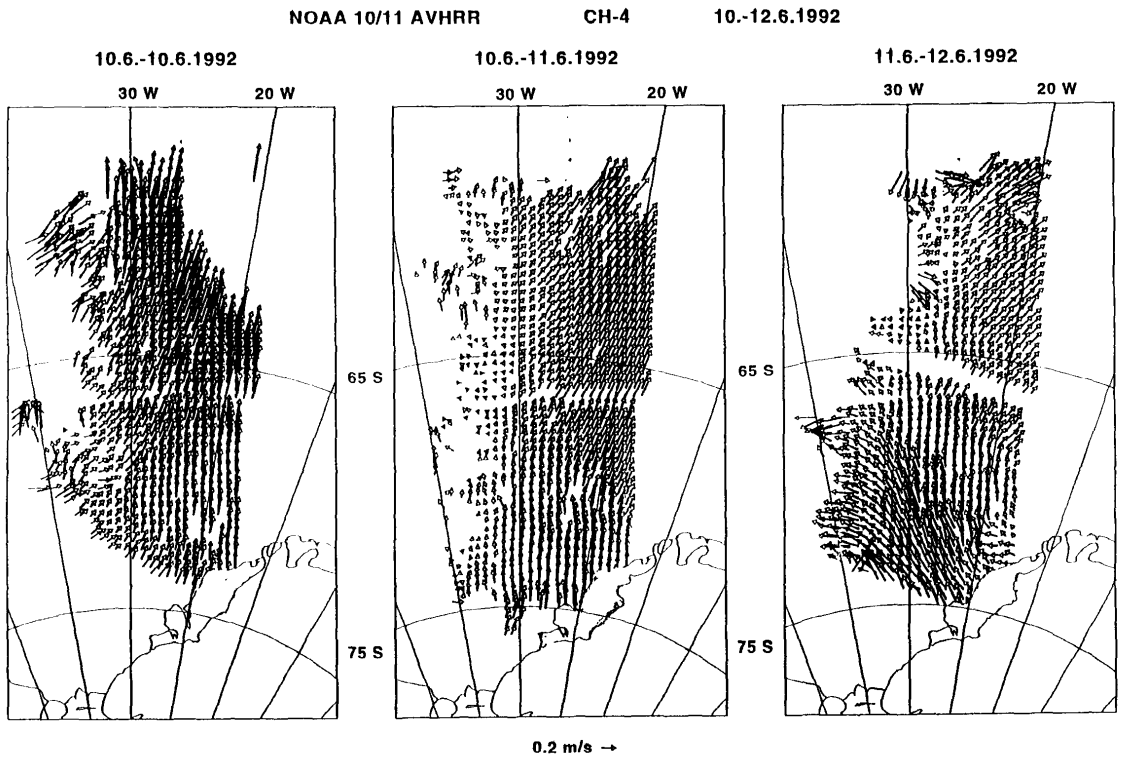

Fig. 2.3-1: Examples of AVHRR derived sea ice velocity fields for the period 10.6-12.6.1992.

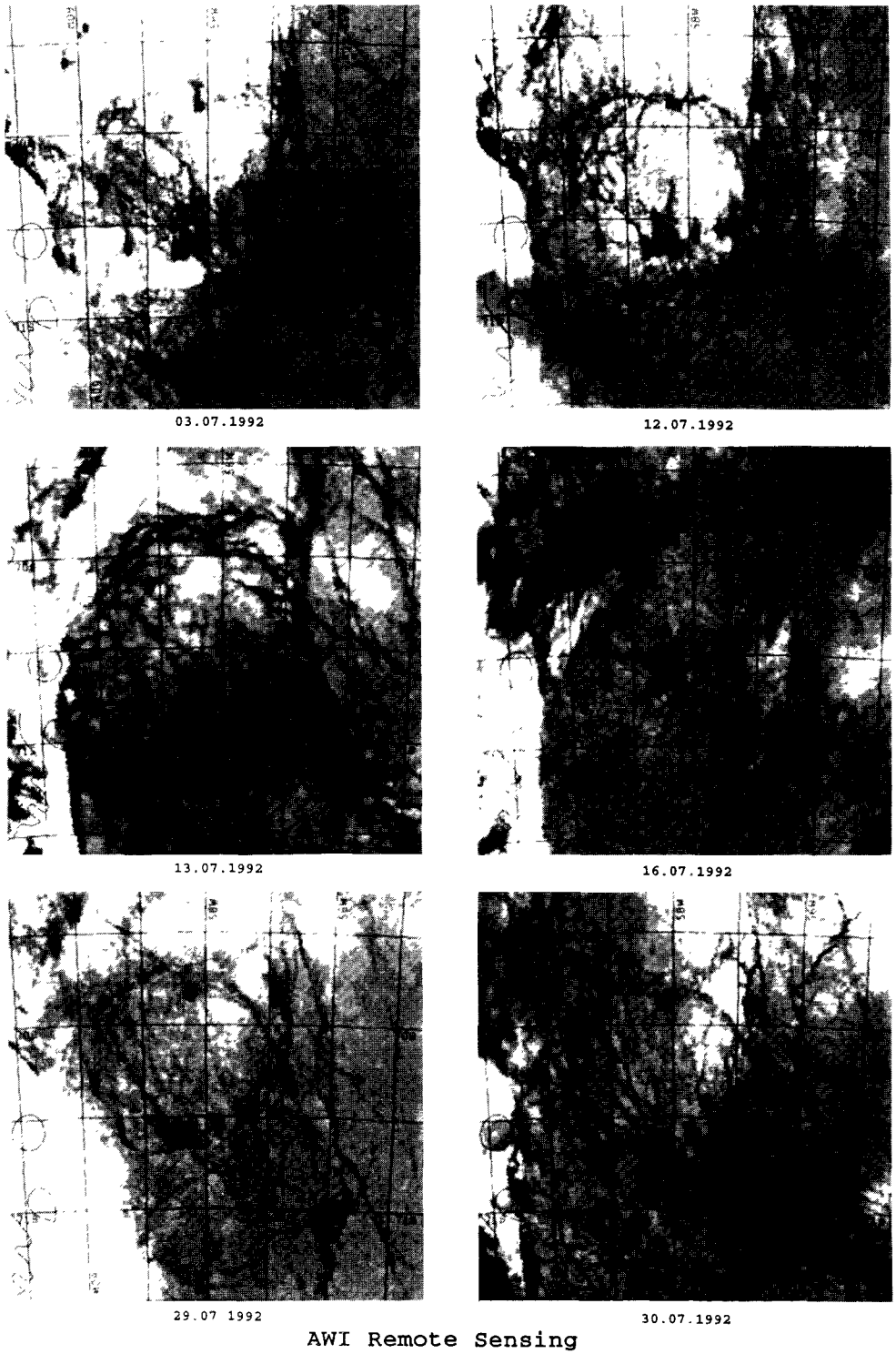

Fig. 2.3-2: Time series of sea ice anomalies in the western Weddell Sea for July 1992 observed by AVHRR infrared sensors. The dark spots represent relatively warm areas (-16˚C to –20˚C) whereas the bright areas have values between –24˚C to –34˚C.

Fig. 2.3-3: Cruise track along the polynya off the shelf ice edge near Atka Bay superimposed over an AVHRR infrared image.

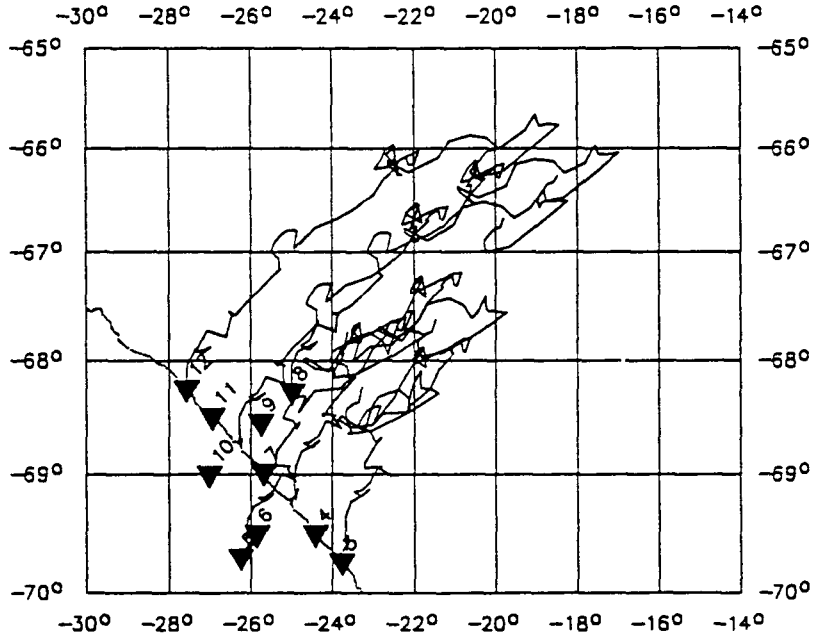

Fig. 2.3-4: Trajectories of the 6 Argos buoys for the period 11.07-01.10.1992 and start positions of the 10 radar reflectors (black triangles).

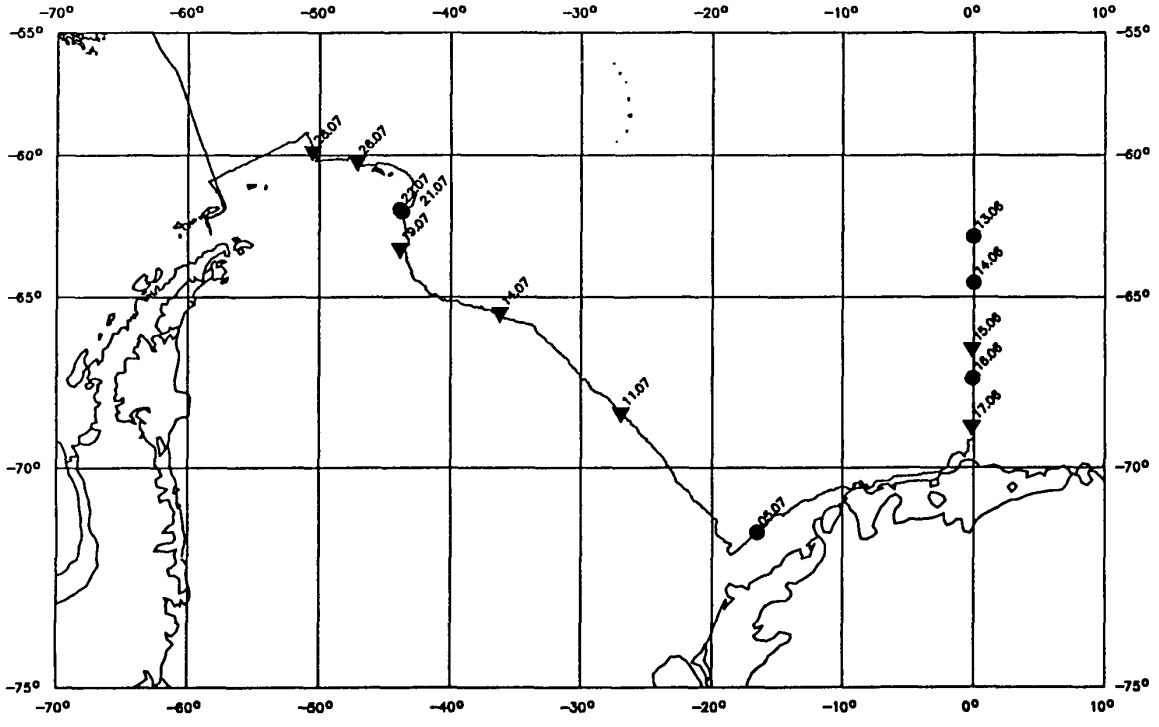

Fig. 2.3-5: Positions of the Video Camera flights (dots) and the combined LineScan Camera/Video Camera flights (triangles).

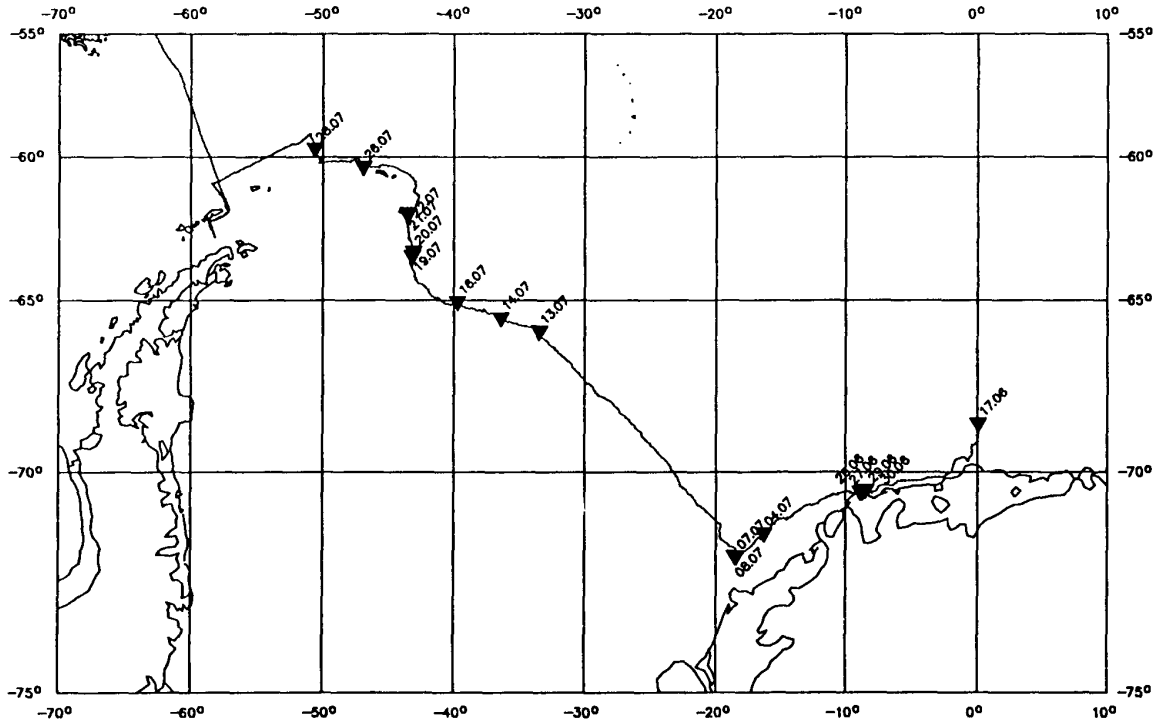

Fig. 2.3-6: Positions of the Laser-Altimeter flights